International Journal of Biological Macromolecules 277 (2024) 134154

Contents lists available at ScienceDirect

International Journal of Biological Macromolecules

journal homepage: www.elsevier.com/locate/ijbiomac

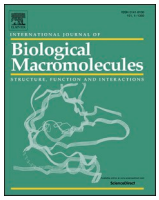

Antimicrobial cyclodextrin-assisted electrospun fibers loaded with carvacrol, citronellol and cinnamic acid for wound healing

Iago Gonzalez-Prada [a], Anabela Borges [b,c], Beatriz Santos-Torres [d], Beatriz Magariños [d], Manuel Simões [b,c], Angel Concheiro [a], Carmen Alvarez-Lorenzo [a,*]

[a] Departamento de Farmacología, Farmacia y Tecnología Farmacéutica, I+D Farma (GI-1645), Faculty of Pharmacy, Institute of Materials (iMATUS), and Health Research Institute of Santiago de Compostela (IDIS), Universidade de Santiago de Compostela, Spain
[b] LEPABE - Department of Chemical Engineering, Faculty of Engineering, University of Porto, Portugal
[c] ALiCE - Associate Laboratory in Chemical Engineering, Faculty of Engineering, University of Porto, Portugal
[d] Departamento de Microbiología y Parasitología, Facultad de Biología, CIBUS, Universidade de Santiago de Compostela, Spain

ARTICLE INFO

Keywords:
Electrospinning
Cyclodextrin
Essential oil components
Antimicrobial
Antioxidant
In ovo CAM test

ABSTRACT

This work aimed to explore an alternative to the use of antibiotics for prevention and treatment of wounds infection caused by two common bacterial pathogens *Staphylococcus aureus* and *Pseudomonas aeruginosa*. For this purpose, three different essential oil components (EOCs), namely carvacrol, citronellol and cinnamic acid, were loaded into electrospun fibers of poly-ε-caprolactone (PCL) aided by alpha-cyclodextrin (αCD) and hydroxypropyl-β-cyclodextrin (HPβCD). Electrospun-fibers prepared with each EOC and their mixtures were screened for antimicrobial capability and characterized regarding morphological, mechanical, thermal, surface polarity, antibiofilm and antioxidant properties. αCD formed poly(pseudo)rotaxanes with PCL and weakly interacted with EOCs, while HPβCD facilitated EOC encapsulation and formation of homogeneous fibers (500–1000 nm diameter) without beads. PCL/HPβCD fibers with high concentration of EOCs (mainly carvacrol and cinnamic acid) showed strong antibiofilm (>3 log CFU reduction) and antioxidant activity (10–50% DPPH scavenging effects). Different performances were recorded for the EOCs and their mixtures; cinnamic acid migrated to fiber surface and was released faster. Fibers biocompatibility was verified using hemolysis tests and *in ovo* tissue integration and angiogenesis assays. Overall, HPβCD facilitates complete release of EOCs from the fibers to the aqueous medium, being an environment-friendly and cost-effective strategy for the treatment of infected wounds.

1. Introduction

Skin and soft tissue infections (SSTIs) are inflammatory microbial invasions of the epidermis, dermis and subcutaneous tissue with a lesion size area of at least 75 cm^2 [1,2]. They occur when skin defenses and microbial invasion interact for different reasons, such as trauma and surgery [3]. SSTIs encompass a wide spectrum of clinical presentations, including cellulitis, impetigo, folliculitis, erysipelas, furuncles and carbuncles [4], with an estimated incidence about 24.6 per 1000 person-year in developed societies [5].

SSTIs range from mild, superficial forms that respond to local care (simple drainage) and oral antibacterial agents, to life-threatening, necrotizing processes, which involve the invasion of deeper tissues, penetrating subcutaneous layers (necrotizing cellulitis), fascia (necrotizing fasciitis) and muscle (pyomyositis and myonecrosis). Underlying diseases may hinder the response to therapy, and complicated wounds require hospitalization, surgical intervention such as drainage and debridement, and parenteral antibacterial therapy. If the treatment is delayed, the mortality rate can be as high as 20–40% [3]. Complicated abscesses, infected burn wounds, infected diabetics ulcers, and deep space wound infections are particularly challenging [1,4]. This scenario has worsened due to the intensive and indiscriminate use of antibiotics, which has induced bacterial resistance against most conventional treatments available [6].

Antimicrobial resistance (AMR) is becoming one of the greatest threats to human health in the 21st century, returning to the level of the pre-antibiotic era [7,8]. It is estimated that by 2050, the AMR mortality rate will balloon to 10 million lives per year at a cost of one hundred trillion dollars. For these reasons, the World Health Organization placed the AMR in the top 10 urgent threats [7]. Most of these infections,

* Corresponding author.
E-mail address: carmen.alvarez.lorenzo@usc.es (C. Alvarez-Lorenzo).

https://doi.org/10.1016/j.ijbiomac.2024.134154
Received 31 May 2024; Received in revised form 14 July 2024; Accepted 23 July 2024
Available online 9 August 2024

including SSTIs, are caused by *Staphylococcus aureus* in Europe (39.9% of isolates) [9] and North America (44.6% of isolates) [10]. *S. aureus* forms part of the common skin microbiome. Traditionally, infections caused by *Staphylococcus* species have responded well to penicillin derivatives, but decades of intensive use produced resistance to β-lactamase (in 1948) and latter to methicillin (MRSA in 1965) and vancomycin (VRSA) [12].

Chronic wounds can also be colonized by the Gram-negative *Escherichia coli* and *Pseudomonas aeruginosa*. *P. aeruginosa* is the second most isolated bacterial specie in North America (11.1% of isolates) and Europe (12.5% of isolates) [9] and the first Gram-negative pathogen in SSTIs. These pathogens belong to the group called ESKAPEE, an acronym of bacteria which are the most dangerous drug-resistant microbes [7]. Therefore, there is an urgent need of developing new approaches to combat AMR [8]. Alternative agents to current antibiotics must meet certain characteristics, such as low toxicity, low risk of inducing resistance, and adequate economic viability [12]. A good alternative that meets these requirements are secondary metabolites synthesized by plants and other organisms necessary for reproduction and the defense mechanisms against other forms of life such as bacteria, fungi, viruses, vertebrates, etc. [8]. These secondary metabolites can be found in essential oils.

Secondary metabolites can be divided into three major categories, namely terpenes, phenolic compounds and nitrogen-containing compounds [8]. These secondary metabolites can be found in essential oils, which are mixtures of 20 to 100 low molecular weight plant secondary metabolites [7]. Essential oils represent a good alternative to the use of antibiotics, since they are not selective. Their hydrophobicity allows them to partition with lipids present in the cell membrane or to bind to the cell surface and penetrate the phospholipid bilayer of bacteria, making the membranes more permeable and disrupting many cellular activities, including energy production (membrane-coupled), membrane transport, and cell metabolism, causing cell death [12,13]. In general, essential oils are less likely to be affected by the resistance mechanisms that bacteria commonly use, such as drug inactivation/alteration, modification of drug binding sites/targets, and changes in cell permeability resulting in reduced intracellular drug accumulation [11].

The non-specific mechanism of action converts essential oil components (EOCs) into broad-spectrum antimicrobial agents, effective against Gram-positive and Gram-negative pathogens [14]. Moreover, most EOCs have antioxidant, anti-parasitic, insecticidal, antiviral, antitumor, and anti-inflammatory capabilities [7,12,15]. Thus, EOCs are versatile and interesting compounds with polyvalent performances. Despite these advantages, there are also numerous constrains that compromise the handling and the effectiveness of EOCs. Generally, EOCs are volatile substances with strong organoleptic flavor, low water solubility and low stability [12]. Therefore, the development of wound dressings or skin scaffolds loaded with EOCs is not straightforward and should consider efficient encapsulation ways that enhance stability and local solubility in order to increase penetration and effectiveness in the skin tissues [16].

This work relies on the hypothesis that electrospun dressings of poly-ε-caprolactone (PCL) containing cyclodextrins (CDs) may act as scaffolds able to encapsulate EOCs and to deliver therapeutic concentrations to the wounds for effective prophylaxis or treatment of infections. Electrospinning is a versatile and economical method to prepare ultrafine fibers with tunable porosity and mechanical properties compatible with soft tissues [17–19]. It can be carried out at room temperature, which is useful to prevent chemical degradation and volatilization of bioactive substances [16,20]. More specifically, the electrospinning technique is especially suitable for the preparation of a wide variety of products for wound treatment, from suture threads with new features to dressings personalized in terms of morphology, composition and ability to monitor the state of the wound [21–23]. PCL is a linear aliphatic semicrystalline polyester of recognized biocompatibility that degrades slowly without altering the surrounding pH, which is an advantage in terms of wound healing compared to other biodegradable polymers [17,24]. Incorporation of CDs may overcome the hydrophobicity of the PCL networks and facilitate the hosting of EOCs by forming inclusion complexes [25–27]. Also, CDs may form poly(pseudo)rotaxanes with a variety of electrospinnable polymers to improve the mechanical properties of the mats, the wettability and the interaction with cells as well as cell proliferation and differentiation [28–30]. Inclusion complexes of EOCs formed during electrospinning can increase the apparent solubility (higher local concentration) and facilitate the diffusion of the EOCs through the soft tissue towards the bacteria [26]. The reports on electrospun fibers containing EOC inclusion complexes are still just a few and mainly intended for fast antimicrobial effect on food preservation [31–34].

To carry out the work, three EOCs of quite different chemical structure, that is, carvacrol (phenolic monoterpenoid), citronellol (monoterpene alcohol) and cinnamic acid (phenolic carboxylic acid), were chosen to evaluate the feasibility of their incorporation into electrospun fibers and to test their antimicrobial capability. Carvacrol is a phenolic monoterpenoid, major component of oregano oil [35], that alters the composition of fatty acids in membrane cell, increasing fluidity and permeability [12], depletes the internal ATP pool of bacterial cells and inhibits the synthesis of flagellin, a microbial protein required for bacterial motility [13]. Carvacrol has been shown to be active against planktonic *S. aureus*, including methicillin-resistant *S. aureus* (MRSA), and *S. epidermidis* as well as Gram-negative bacteria [36]. It is classified as fast acting compound, an important quality for obtaining a good response in the first hours of infection [12]. Citronellol is a monoterpene alcohol found in the essential oil of plants of the genus *Cymbopogon*, which can modify the hydrophobicity and disrupt bacteria membrane integrity, leading to the leakage of K^+ ions [13,15,37]. Cinnamic acid is a phenolic carboxylic acid found in several plants such as *Cinnamomum cassia* and *Panax ginseng*, which exhibits antioxidant, antimicrobial, anticancer, neuroprotective, anti-inflammatory and antidiabetic properties [38]. It is active against both planktonic and sessile forms of *S. aureus*; the reduction of sessile bacteria being comparable to that of peracetic acid and sodium hypochlorite and more efficient than that of hydrogen peroxide [39,40]. Cinnamic acid can cross the cell membrane by passive diffusion as undissociated acid (pKa ≈ 4.2), disturb or even disrupt the cell membrane structure, acidify the cytoplasm and cause denaturation of proteins [39].

The aim of this work was to obtain a resistant but flexible electrospun scaffold that allows the patients mobility while not deteriorating, carrying a high content in EOCs to provide antibiofilm, angiogenic and antioxidant activity and be used as safer and cost-effective alternative to antibiotics. Several mixtures of PCL with alpha-cyclodextrin (αCD) and hydroxypropyl-β-cyclodextrin (HP-β-CD) were first prepared, and adequate solvents for electrospinning of the mixtures were identified. In terms of safety, the chosen cyclodextrins show an excellent safety profile whether administered dermally or parenterally and are easily cleared from the body by renal filtration if they enter the bloodstream [41]. Morphological, mechanical, thermal and surface properties of the fibers were investigated. Then, fibers loaded with selected EOCs were tested for their preventive action on *S. aureus* and *P. aeruginosa* biofilm set-up, as well as antioxidant and anti-inflammatory properties. Additional studies were also conducted with fibers prepared with binary and ternary combinations of EOCs in an attempt to enhance the antimicrobial efficiency [42] while still preserving biocompatibility.

2. Materials and methods

2.1. Materials

Poly-ε-caprolactone (PCL) (80 kDa), 1-bromonaphthalene, carvacrol and 2,2-diphenyl-1-picrylhydrazyl (DPPH) were purchased from Sigma-Aldrich (Steinheim, Germany). Citronellol and cinnamic acid were from Acros (Waltham, MA, USA). Alpha-cyclodextrin (α-CD) Cavamax W6

was from Wacker Chemie (Munich, Germany) and hydroxypropyl-β-cyclodextrin (HPβCD) was purchased from Roquette (Lestrem, France). Tetrahydrofuran (THF), dimethylformamide (DMF) and Live/Dead™ *Bac*Light™ Bacterial Viability Kit were provided by Thermo Fisher Scientific (Waltham, MA, USA). Phosphate-buffered saline (PBS) pH ~7.4 medium was prepared as indicated in the European Pharmacopoeia 6th edition, mixing 8 g/L NaCl, 2.38 g/L Na_2HPO_4 and 0.19 g/L KH_2PO_4 in ultrapure water. Mueller-Hinton (MH) medium was from Oxoid (Hampshire, UK), Luria-Bertani (LB) from Liofilchem (Roseto degli Abruzzi, Italy), plate count agar (PCA) from Merck (Darmstadt, Germany) and formamide from Merck (Darmstadt, Germany). Acetonitrile and ethanol were provided by VWR Chemicals (Leuven, Belgium). Paraformadehyde 3.7–4% was from Panreac (Castellar del Vallès, Barcelona, Spain). Ultrapure water (resistivity > 18.2 MΩ cm; Milli-Q®, Millipore Ibérica, Madrid, Spain) was obtained by reverse osmosis.

2.2. Preparation of electrospinning solutions

PCL (1.5 g) was dissolved in a mixture of 6 mL of THF and 4 mL of DMF at 45 °C under stirring for 6 h to obtain a 15% PCL solution. Preliminary tests with PCL of 50 kDa were done with PCL concentrations up to 30%. Subsequent tests with PCL of 80 kDa were carried out with 8% (preliminary test), 12%, 15%, 18%, 20% and 22% PCL solutions. When the dispersion reached room temperature, carvacrol, citronellol or cinnamic acid were added in various amounts to cover a wide range of concentrations, i.e., 1%, 2%, 5%, 10%, 20% and 30% (*w/v*). The dispersions remained overnight under gentle agitation.

PCL (80 kDa)/αCD fibers were prepared in two steps. PCL (1.5 or 1.8 g) was dissolved in 6 mL of THF and heated at 45 °C with stirring for 24 h. In separate, αCD (0.2, 0.5, 0.7 and 1 g) was dissolved in 4 mL of DMF under stirring for 24 h at room temperature. Then, α-CD/DMF solutions were added to the PCL/THF solutions with stirring. The mixture was magnetically stirred (200 rpm) at room temperature for 7 days. Once a homogeneous dispersion was obtained, the EOC was added at room temperature with gentle stirring overnight.

PCL (80 kDa)/HPβCD fibers preparation followed the same steps as for PCL/αCD, except for the use of 1.5 g PCL and 0.7 g HPβCD instead of αCD.

2.3. Electrospinning process

A climate-controlled Yflow® Professional Electrospinning Machine (Yflow® S.D., Málaga, Spain) was used for fibers preparation. A series of experiments were carried out varying the electrospinning parameters to optimize the process. The applied voltages ranged between 10 and 15 kV, the collection distance was set at 25.0 cm, and the feeding rates were 1.0–2.0 mL/h for αCD and HPβCD. Composition and electrospinning conditions for each fiber are summarized in Table S1 (Supplementary Material file).

2.4. Biofilm prevention studies of the electrospun mats

2.4.1. Biofilm cells culturability

The activity of the electrospun nanofiber mats was assessed on preventing *S. aureus* (strains CECT 976 and ATCC 25923) and *P. aeruginosa* (CECT 110) biofilm set-up (24 h biofilms formed in the presence of electrospun nanofiber mats) following a modification of the AATCC 100–Test Method for Antibacterial Finishes on Textile Materials. These strains are commonly used as model to validate the antimicrobial and antibiofilm activity of natural-based molecules [43,44]. Briefly, the nanofiber mats were cut into square pieces of 1.0 cm × 1.0 cm (≈10 mg) and sterilized under UV light for 30 min per side. The sterilized fibers were placed in a sterile 24 well polystyrene microtiter plate (Orange Scientific, Braine-l'Alleud, Belgium). Then, bacterial suspension (2 mL) of *S. aureus* in MH broth (0.04 optical density at 620 nm) or *P. aeruginosa* in LB broth (0.04 optical density at 620 nm) was prepared and added to each well and incubated for 24 h at 37 °C under mild stirring (100 rpm). After that contact time, the fibers were removed and placed in 2 mL PBS (pH = 7.4) in falcons and shaken using a vortex for about 1 min. Subsequently, 100 μL of the falcon solution was transferred to an Eppendorf with 900 μL of PBS and 10-fold serial dilutions were conducted. For each dilution factor, 20 μL were spread on PCA plates and incubated at 37 °C for 24 h. After the incubation period the number of colony forming units (CFU) were counted and expressed as CFU/mL using Eq. (1) [43].

$$\frac{CFU}{mL} = \frac{N}{SV \times Dilution} \quad (1)$$

where *N* is the number of CFU on the PCA plates and *SV* is the sample volume in mL.

Four replicate experiments were performed for each sample, testing two replicates in different weeks and the growth reduction was evaluated according to the Japanese Industrial Standard, as follows: no antimicrobial activity (<0.5 log microbial growth reduction), slight antimicrobial activity (0.5 to 1 log microbial growth reduction), significant antimicrobial activity (1 to 3 log microbial growth reduction) and strong antimicrobial activity (>3 log microbial growth reduction) [45].

2.4.2. Biofilm cells membrane integrity

The selective staining exclusion method was used to evaluate the integrity of the biofilm cells membrane of *S. aureus* (strain CECT 976) following the method of Oliveira et al. [46]. For this assay, the Live/Dead BacLight™ kit (Invitrogen, USA) was used, which comprises two nucleic acid binding stains, SYTO 9™ and propidium iodide (PI). The green fluorescent SYTO 9 is capable to penetrate all cell membranes and stains the cells green, whereas fluorescent red PI is assumed to penetrate only cells with damaged cytoplasmic membranes and stains the cells red. For this, after the biofilms grown during 24 h on PCL and PCL/αCD mats, the fibers were removed, transferred to falcons containing PBS and vortexed (as described in Section 2.4). Then, 700 μL of each bacterial suspension was stained with 250 μL SYTO9™ and 50 μL PI, allowed to react in the dark for 7 min, and the resulting mixture filtered through a black polycarbonate membrane (Whatman International Ltd., Maidstone, UK). Then, the membranes were mounted on a microscope slide, and the samples visualized with a LEICA DMLB2 epifluorescence microscope (LEICA Microsystems Ltd., Weltzlar, Germany), and photos were taken for a subsequent analysis.

2.4.3. Biofilm cellular density

PCL/HPβCD nanofiber mats were cut as square pieces of 1.0 cm^2, sterilized under UV light for 30 min per side, and placed in a sterile 24 well-plate. Then, bacterial suspension of either *S. aureus* (ATCC 25923) in MH medium or *P. aeruginosa* (CECT 110) in LB medium (2 mL) was added to each well and incubated for 24 h at 37 °C under slight stirring (100 rpm). After that contact time, the fibers were removed and placed in 2 mL PBS, pH = 7.4. Then 500 μL of SYTO 9/PBS (0.5% *v*/v) and 500 μL of PI/PBS (0.5% v/v) were added directly to the well with the fiber. The dyes were allowed to react for 15 min in the dark. Then, the fibers were removed from the wells with the help of tweezers, mounted on a slide and analyzed under a Leica STELLARIS 5 confocal microscope (Leica Microsystems, Germany). LAS X® version 3.7.4.23463 (2020 Leica microsystems CMS GmbH) image processing and archiving software were used to acquire the images. A total of 20 fields were counted and at least three independent membranes were used to calculate total cells per square centimeter of biofilm.

2.5. Fibers characterization

Electrospun mats were coated by sputtering iridium under argon (Sputter Coater (Ir) - QUORUM Q150T-S) and observed using a ZEISS FESEM ULTRA Plus (Carl Zeiss, Oberkochen, Germany). The average

diameter of 150 measurements made in 4–6 different areas of each electrospun mat was recorded using the ImageJ analysis software.

Mechanical properties of each type of fibers were investigated using a TA.XT plus Texture Analyzer (Stable Micro Systems, Surrey, UK) equipped with a 30 Kgf (~294 N) load cell under a crosshead speed of 10 mm/min. The fibers were cut as square pieces of 2.0 cm × 2.0 cm. Ten specimens were tested and the Young's modulus was calculated as the slope of the linear (elastic) region of the stress-strain curve.

X-ray powder diffraction (XRPD) pattern of PCL, αCD and HPβCD and the different fibers without EOCs were recorded to verify the formation of inclusion complexes between PCL and CDs. A Philips powder diffractometer fitted with a PW1710 control unit, a PW1820/00 goniometer and an Enraf Nonius FR590 generator was used. Spectra were made by measuring the scintillation response to Cu Kα radiation in the 2–50° 2θ range, with a step size of 0.04° and counting time of 6 s per step.

Differential scanning calorimetry (DSC) scans of the raw materials and the fibers with and without EOCs were performed using a Q100 DSC (TA Instruments, New Castle, DE, USA). The specimens were accurately weighed in a 40 μL aluminum pan, covered with a tap, and then heated from 25 to 65 °C, cooled to −20 °C and then heated to 300 °C at a scanning rate of 10 °C/min in nitrogen atmosphere (50 mL/min).

Contact angles of water, formamide and 1-bromonaphthalene on the electrospun mats were measured using a OCA 15 Plus contact angle system (Dataphysics Instruments, Germany), fitted with a videocamera that allowed for image acquisition and data analysis, following a previously described protocol [47]. Fiber pieces (1 cm × 6 cm) were glued to a glass slide with double-sided tape. For each fiber sample, 6 to 10 measurements were made at room temperature (23 ± 2 °C). Hydrophobicity was evaluated after contact angles measurement following the van Oss' approach [48–50]. The surface tension components of the solvents were obtained from literature [51].

2.6. EOC release tests

PCL and PCL/HPβCD fibers (1–30 mg) were immersed in vials containing PBS (pH 7.4) 10–25 mL (depending on the mass of the samples) and placed in a mini-shaker (VWR) at 37 °C and 100 rpm. At predetermined times, aliquots from the release medium were taken, replaced with same volume of fresh medium and filtered (Scharlau® Syringe Filter, 0.22 μm 13 mm PTFE hydrophilic). The concentration in EOC was quantified by HPLC (AS-4140 autosampler, PU-4180 pump, LC-NetII/ADC interface box, CO-4060 column oven, MD-4010 photodiode array detector, JASCO, Tokyo, Japan) fitted with a C18 column (Waters Symmetry C18, 5 μm, 4.6 × 250 mm) and operated with ChromNAV software v.2. The mobile phase was used in a gradient elution. Briefly, the mobile phase was initially set as water:acetonitrile in the ratio 70:30 (*v*/v) and then linearly changed to 20:80 (v/v) over 15 min. Eluent was pumped at flow rate of 1 mL/min and the sample injection volume was 30 μL. Carvacrol was quantified at a wavelength of 276 nm (retention time 10.56 min), citronellol at 210 nm (retention time 11.11 min) and cinnamic acid at 270 nm (retention time 2.01 min). The detection limit (LOD) and the quantification limit (LOQ) were determined for each EOC, as follows: carvacrol 0.381 ppm and 1.154 ppm, citronellol 1.177 ppm and 4.173 ppm, and cinnamic acid 1.848 ppm and 4.909 ppm, respectively. The experiments were carried out in triplicate. HPLC calibration curves of each EOC are shown in Figs. S1 to S3 in Supplementary Material.

2.7. Antioxidant activity

The antioxidant activity was determined using the DPPH free radical method. A 24-hour release study was performed at 37 °C and 100 rpm, immersing the fibers in 2 mL of PBS. Release medium samples (200 μL) were taken at stablished time points. DPPH solution (200 μL; 80 μg/mL) in ethanol:PBS 50:50 (*v*/v) was added to each aliquot of the fiber release medium, and the mixtures were kept protected from light and oxygen. After 2 h at 37 °C and 100 rpm, the absorbance was recorded at 517 nm by UV spectrophotometry (Agilent 8453, Boeblingen, Germany).

Control experiments were carried out with fresh carvacrol, citronellol and cinnamic acid solutions obtained from a previously prepared high concentration stock solution. To this end, 1000 mg of EOC were diluted in 1 mL of DMSO. Then, 60 μL of each stock solution were taken and added to 1940 μL of ethanol:PBS 50:50 (*v*/v) to obtain a final concentration of 30 mg/mL. For preparing 11 serial dilutions, 1.4 mL were taken from this solution and mixed with 400 μL of ethanol:PBS 50:50 (v/v). Finally, for each dilution factor, 400 μL was taken and mixed with 400 μL of a previously prepared DPPH stock solution (4 mg/100 mL of ethanol:PBS 50:50 (v/v)). After mixing each diluted solution with DPPH solution, all prepared solutions were agitated at 100 rpm and 37 °C for 2 h with protection from light. Then, the absorbance was recorded at 517 nm by UV spectrophotometry.

2.8. Hemolysis test

Square pieces of fibers (1 × 1 cm) were hydrated with PBS (pH 7.4) for 2 h and placed in Eppendorf tubes. A blood stock solution was prepared by diluting 6.25 mL of total volunteers' blood (Galician Transfusion Center, Spain) previously anticoagulated with EDTA in 250 mL of PBS (pH 7.4). Aliquots (1.5 mL) of the stock solution were added to each Eppendorf. After incubation for 1 h at 37 °C in a minishaker, the tubes were centrifuged at 10,000*g* for 10 min [52]. The supernatant (150 μL) was taken and placed in 96 well plate.

The hemolytic activity was calculated as a function of the released hemoglobin, which was measured by recording the absorbance (Abs) of the supernatant using a UV–visible microplate reader (Testal, Germany) at 510 nm. Triton 1% solution was used as the positive control (PC) (100% lysis) and blood stock solution was used as the negative control (NC). The hemolysis percentage was calculated using Eq. (2):

$$\%Hemolysis = \frac{(Abs_{sample} - Abs_{NC})}{(Abs_{PC} - Abs_{NC})} \times 100 \quad (2)$$

2.9. In ovo tissue integration and angiogenesis evaluation

Fertilized hen eggs were supplied by Coren (San Cibrao das Viñas, Spain) and placed in an incubator at 37 °C and 60% relative humidity (Incubato IN-EI-528; Expondo, Zielona Góra, Poland). The position of the eggs was changed (180°) three times per day to mimic the movements by the hen. Lapsed 3 days, a small window (1 × 1 cm) was opened with a scalpel and scissors to verify that the eggs were fertilized and in optimal conditions to continue with the test. Moreover, this window provoked the retraction of the chicken chorioallantoic membrane (CAM) creating a greater empty space, facilitating the incorporation the scaffolds in the following days. The window was covered with a piece of parafilm to prevent contaminating agents from invading the internal part of the eggs, which were placed back in the incubator in an upright position until day 8. Then, the state of the egg was checked, and the fibers previously sterilized by UV and cut into 8 mm circles (with the help of a punch) were incorporated. Two fibers of the same type were placed in each egg to reduce the number of eggs used. The experiment was done in quadruplicate for each fiber composition. The window was closed again.

On day 12, after 5 days of contact of the fibers with the CAM, tissue integration and angiogenesis were evaluated. First, the parafilm was removed and the size of the window was increased using scissors. Then, the CAM was fixed by adding a few drops of 3.7–4% paraformadehyde until the entire surface was covered. After 3 h, the membrane was well fixed and the perimeter of CAM in contact with the fibers was cut. The fiber-CAM system was washed three times with PBS and placed on a slide to obtain the corresponding images with the help of a stereo microscope with an integrated SZ-CTV camera (Olympus, Japan). Finally,

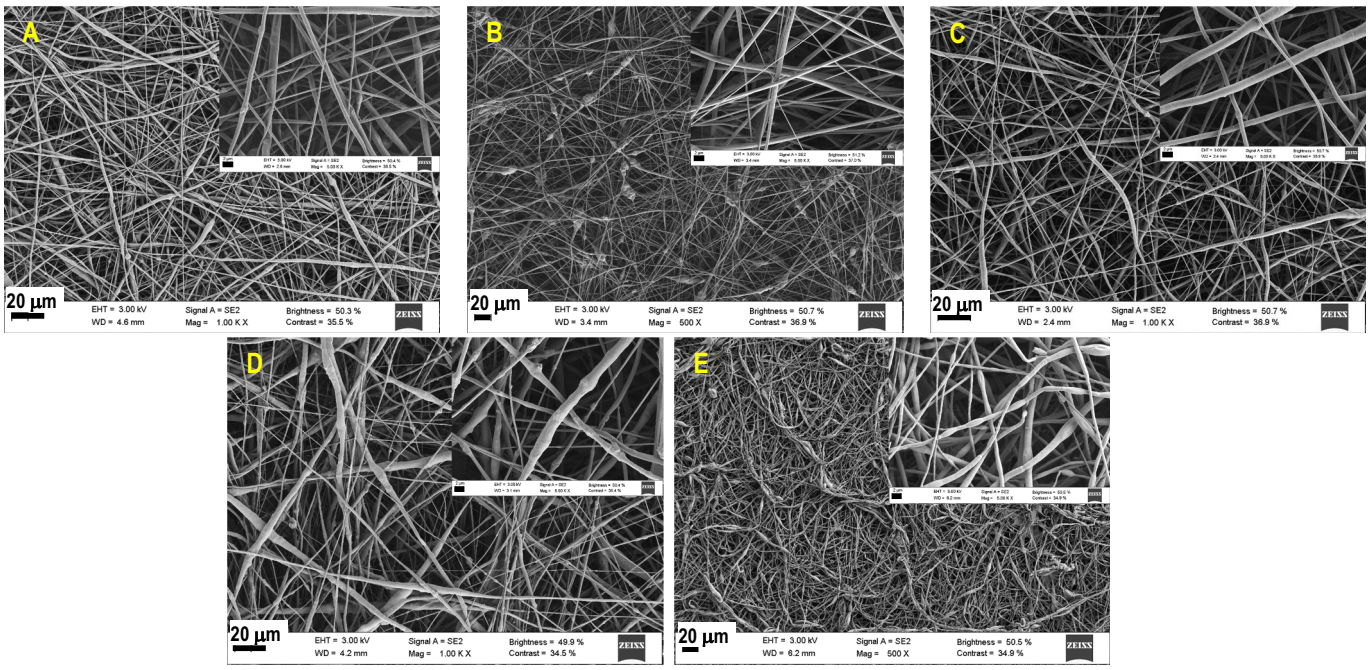

Fig. 1. FESEM images recorded at 500× and 1000× (scale bar 20 μm), with inserts at 5000× magnification (scale bar 2 μm) of electrospun mats: A) PCL (80 kDa) 15% (*w/v*) αCD 2% (w/v) THF:DMF (60:40); B) PCL (80 kDa) 15% (w/v) αCD 7% (w/v) THF:DMF (60:40); C) PCL (80 kDa) 18% (w/v) αCD 2% (w/v) THF:DMF (60:40); D) PCL (80 kDa) 18% (w/v) αCD 7% (w/v) THF:DMF (60:40); and E) PCL 15% HPβCD 7% (w/v) THF:DMF (50:50).

the images were analyzed using the ImageJ program to determine the area occupied by the vessels in contact with the fibers. A score of integration (SI) was given to each scaffold, based on the neovascularization and attachment of the scaffold to the CAM. This score ranged from 0 (poor integration) to 3 (excellent integration) [53].

2.10. Statistical analysis

Statistical analysis was performed using SPSS v.26.0 (IBM Co., Armonk, NY, USA). All results were expressed as mean ± standard deviation. Statistical analyses of the antimicrobial and antioxidant results (one-way ANOVA) were conducted, followed by the post hoc Tukey HSD multiple comparison test. Previously statistical analysis normality of all variables was evaluated using Kolmogorov-Smirnov test for groups ($n \geq 50$) and Shapiro–Wilk test for groups ($n \leq 50$). A confidence interval was used at least 95%, to define statistical significance ($^{*}p < 0.05$, $^{**}p < 0.005$, $^{***}p < 0.001$ and $^{****}p < 0.0001$).

3. Results and discussion

EOCs may offer a variety of performances during wound healing, but this study was particularly focused on their capability to prevent/treat infections as an alternative to the use of conventional antibiotics. Thus, the first steps were devoted to find the best conditions to incorporate sufficiently higher amounts of EOCs in electrospun nanofibers by either increasing the concentration in PCL or adding cyclodextrins that can modulate the mechanical properties of the fibers (mainly αCD) and form inclusion complexes with the EOCs (mainly HPβCD). Then, the electrospun fibers were first challenged against biofilm formation, which is a major concern for chronic wound healing. Detailed structural and mechanical characterization and EOC release pattern of the fibers was carried out to find correlations with their biofilm prevention performance. Finally, biocompatibility of the most potent antibiofilm and antioxidant electrospun mats was preliminary screened in an *in ovo* model stablished as a suitable alternative to in vivo testing.

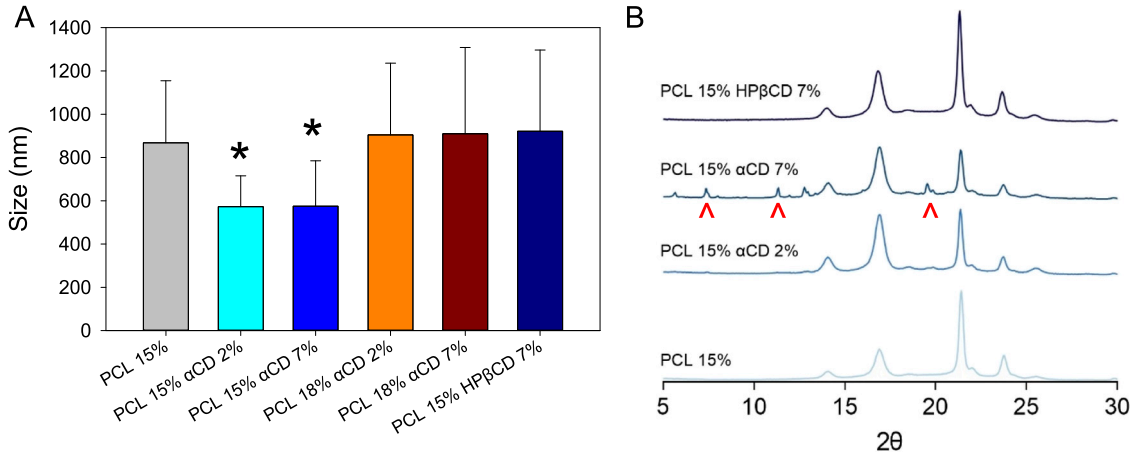

Fig. 2. (A) Diameters ($n = 50$) and (B) X-ray diffractograms of PCL fibers prepared with different contents in αCD and HPβCD. Red symbols in plot B indicate the peaks typical of free αCD at 7 and 12°2θ and of crystalline poly(pseudo)rotaxane aggregates formed by αCD at 20°2θ.

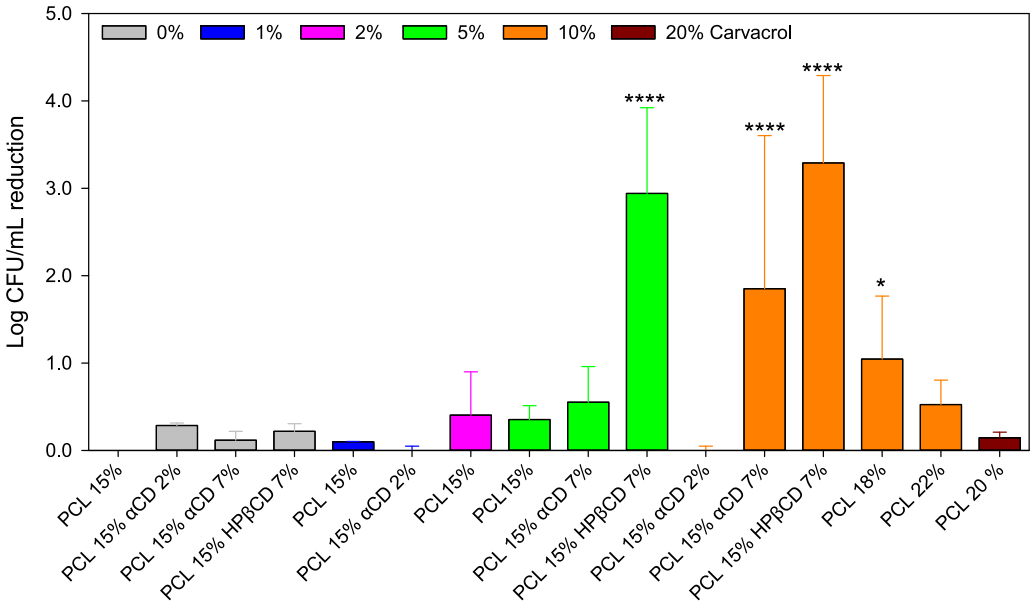

Fig. 3. Preventive action of PCL, PCL-αCD and PCL-HPβCD fibers loaded with carvacrol at different concentrations (from 1 to 20%, as indicated in the legend) against *S. aureus* biofilms, in terms of reduction of culturable cells (log (CFU/mL) reduction) after 24 h contact time. Mean ± standard deviation, $n = 4$, $^{*}p < 0.05$, $^{**}p < 0.005$, $^{***}p < 0.001$ and $^{****}p < 0.0001$.

3.1. Fibers preparation

Preliminary studies were carried out with solutions prepared with PCL varieties of different molecular weight (50 kDa and 80 kDa) and covering a wide range of concentrations. The use of PCL with a molecular weight of 50 kDa generated irregular fibers of very diverse sizes (Fig. S4 in Supplementary Material). To overcome this drawback, PCL with a molecular weight of 80 kDa was chosen. Different concentrations of PCL (8%, 12%, 15% and 18%) were tested in THF:DMF 60:40 *v*/v mixtures. Solutions of 8% PCL rendered nanofibers with beads throughout the entire fibers (Fig. S4c). Differently, 12% PCL solutions allowed obtaining continuous, smooth, homogeneous fibers without beads (Fig. S4d). Image analysis performed using Image J software showed diameters of 830 ± 250 nm according to normal distribution (Fig. S5 in Supplementary Material).

PCL (80 kDa) and αCD nanofiber mats were successfully electrospun from dispersions containing 15% of PCL and 2–7% of αCD (Fig. 1). At the time of mixing the two dispersions, the system was transparent, but the two dispersions were perfectly distinguishable (probably due to a difference in density), and after 24 h of stirring the dispersion was completely white suggesting an interaction between PCL and αCD [54]. PCL 15% αCD 2% nanofiber mats were composed of continuous, cylindrical fibers, of average diameters of 572.6 ± 142.9 nm (Fig. 2A). Increasing the amount of αCD in the polymer dispersion, some beads appeared along some fibers, but did not cause an increase in the fiber diameter. PCL 15% αCD 7% fibers had average diameter of 574.9 ± 209.9 nm ($n = 50$), like PCL 15% αCD 2% fibers (Figs. S6–S10). However, the PCL 15% αCD 7% fibers were more heterogeneous in size and their surfaces showed some lumps and bumps, as previously observed for poly(pseudo)rotaxane-containing fibers [25]. PCL 18% αCD 2% fibers had average fiber diameters of 904.2 ± 331.5 nm (n = 50). PCL 18% αCD 7% fibers had diameters of 909.6 ± 398.9 nm (n = 50). Compared to PCL 15% fibers, an increase in PCL concentration to 18% caused an increase in fibers diameter, and the addition of αCD did not induce bead formation. Differently, the incorporation of HPβCD 7% (*w*/*v*) to PCL 15% (w/v) solution did not cause changes in size (921.5 ± 375.2 nm) compared with the control PCL 15% fibers (Fig. 2A). The different effects of αCD and HPβCD on the fibers diameter can be attributed to differential interactions of PCL with these cyclodextrins. αCD can tread along PCL chain forming a poly(pseudo)rotaxane as also observed by other authors [25,28] causing the aggregation of PCL chains, as further investigated by X-ray diffraction (Fig. 2B). Meanwhile, the treading of HPβCD is less favorable due to the larger size of the cavity, and most HPβCD is expected to remain free lengthwise the fiber forming nanowebs [55]. The weight % of PCL was similar, although slightly higher than that previously used in related papers, but the weight % of αCD tested was in the middle range of those investigated by Tonelli's group [25]. In good agreement with previous reports, the dispersions containing poly(pseudo)rotaxanes were slightly more viscous than PCL-only solutions but still perfectly workable and electrospinnable.

XRP diffractograms of PCL 15%, PCL 15% αCD 2%, PCL 15% αCD 7% and PCL 15% HPβCD 7% fibers are shown in Fig. 2B. PCL is semi-crystalline (60% crystallinity with an orthorhombic crystal structure) and has strong characteristic peaks at 14, 16, 22 and 24°2θ. The fibers maintained those peaks. Poly(pseudo)rotaxane formation with αCD was evidenced as a new peak at 20°2θ due to its columnar packing, which was not observed for a physical mixture of PCL and αCD [25]. Clearly, this peak was more intense in the fibers with the highest content in αCD, in good agreement with literature [54]. In addition, PCL 15% αCD 7% fibers showed peaks at 7 and 12°2θ which may correspond to free αCD (native cage state) probably due to an excess of αCD not interacting with PCL. Differently, the fibers with HPβCD 7% did not show any additional peak, indicating that the interactions between both PCL and HPβCD, if any, are weak and do not increase the crystallinity of the fibers. This means that this cyclodextrin can remain free to form inclusion complexes with the EOCs. Lower contents in HPβCD were not tested aiming to have sufficiently cyclodextrins to accommodate the EOCs.

3.2. Antibiofilm activity

Once the concentration of PCL and cyclodextrins and the electrospinning conditions were set, fibers were prepared with the EOCs and their antibiofilm activity (in terms of biofilm cells culturability) was screened before further assessment.

3.2.1. *S. aureus* biofilm prevention

The MIC and MBC of *S. aureus* have been reported to be 0.128 and

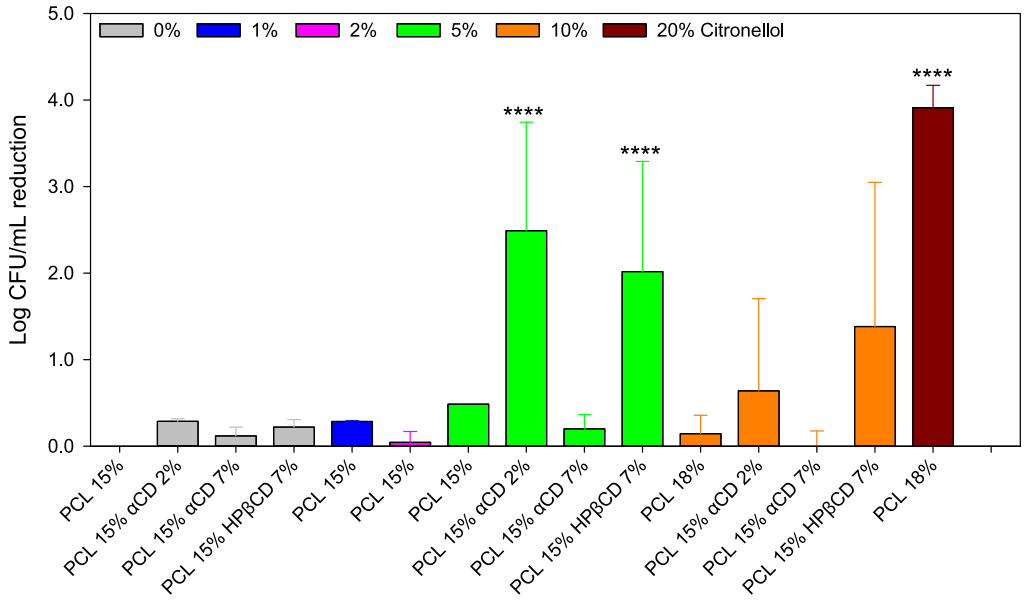

Fig. 4. Preventive action of PCL, PCL-αCD and PCL-HPβCD fibers loaded with citronellol at different concentrations (from 1 to 20%, as indicated in the legend) against *S. aureus* biofilms, in terms of reduction of culturable cells (log (CFU/mL) reduction) after 24 h contact time. Mean ± standard deviation, $n = 4$, $^{*}p < 0.05$, $^{**}p < 0.005$, $^{***}p < 0.001$ and $^{****}p < 0.0001$.

0.512 mg/mL for carvacrol [56], 0.375 and 0.400 mg/mL for citronellol [37] and 6.25 and 25 mg/mL for cinnamic acid [57].

PCL 15% fibers with concentrations of 1%, 2% or 5% of carvacrol did not trigger antibiofilm effects against *S. aureus* (Fig. 3). The next step was to increase the concentration of PCL to 18%, 20% and 22% (*w/v*) to encapsulate a greater amount of carvacrol (up to 20% (w/v)) but minor improvements in biofilm prevention properties (0.5–1 log CFU/mL reduction) were obtained, probably due to an inefficient release of carvacrol (the fibers were fused together). To overcome this problem, αCD was incorporated into the fibers in different amounts: 2% and 7% (w/v).

The fibers with αCD 2% did not show antibacterial activity (<0.5 log CFU/mL reduction) while the fibers with αCD 7% showed a slight microbial activity (0.5–1 log CFU/mL reduction). No statistical differences were observed when carvacrol 5% was included in the fibers. Incorporation of carvacrol at higher proportions improved the antimicrobial activity; PCL 15% αCD 7% carvacrol 20% caused 1–3 log CFU/mL reduction ($p < 0.0001$, with respect to the control fibers and fibers without cyclodextrins). Nevertheless, fibers prepared with αCD 7% showed high variability in the antimicrobial performances (Fig. 3). Thus, it was replaced by HPβCD at 7%. Fibers incorporating HPβCD 7% showed strong antimicrobial activity (>3 log CFU/mL reduction) and presented great improvements ($p < 0.0001$) with respect to the fibers prepared with 5% and 10% carvacrol. These results suggested that the fibers require a carvacrol concentration of 5% or higher and that an effective release of carvacrol from the fiber should be ensured, which could be provided by HPβCD as verified in subsequent sections.

Similar results were observed for PCL 15% fibers containing 1%, 2%,

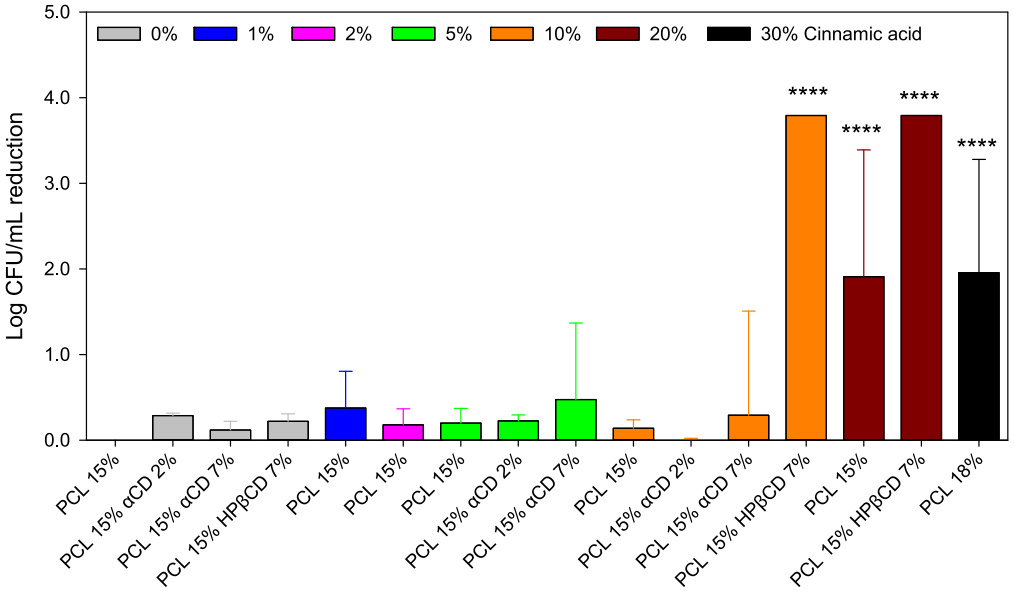

Fig. 5. Preventive action of PCL, PCL-αCD and PCL-HPβCD fibers loaded with cinnamic acid at different concentrations (from 1 to 30%, as indicated in the legend) against *S. aureus* biofilms, in terms of reduction of culturable cells (log (CFU/mL) reduction) after 24 h contact time. Mean ± standard deviation, $n = 4$, $^{*}p < 0.05$, $^{**}p < 0.005$, $^{***}p < 0.001$ and $^{****}p < 0.0001$.

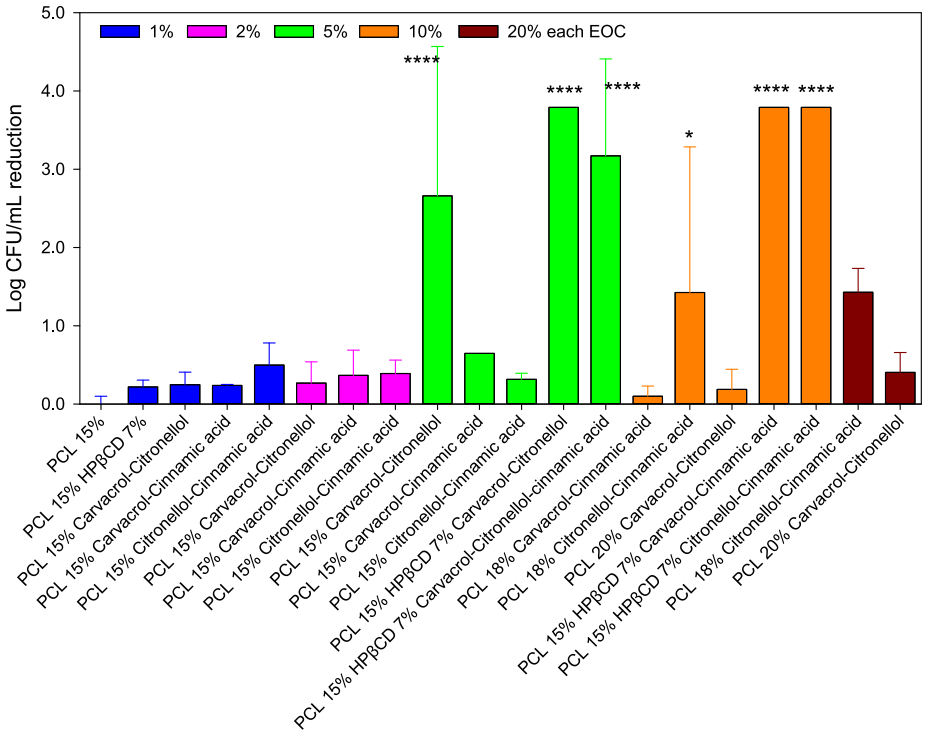

Fig. 6. Preventive action of PCL, PCL-αCD and PCL-HPβCD fibers loaded with binary (1:1) and ternary (1:1:1) mixtures of carvacrol, citronellol and cinnamic acid (from 1 to 20%, as indicated in the legend) against *S. aureus* biofilms, in terms of reduction of culturable cells (log (CFU/mL) reduction) after 24 h contact time. Mean ± standard deviation, $n = 4$, $^{*}p < 0.05$, $^{**}p < 0.005$, $^{***}p < 0.001$ and $^{****}p < 0.0001$.

or 5% (*w/v*) of citronellol, indicating the lack of antimicrobial properties due to either an inefficient release of the EOC (PCL forms a hydrophobic network) or an insufficient content of citronellol (Fig. 4). PCL 18% fibers that were prepared containing 10% citronellol did not display antimicrobial activity either. Differently, PCL 18% citronellol 20% showed a strong antimicrobial activity (>3 log CFU/mL reduction; $p < 0.0001$).

PCL 15% with αCD fibers were prepared in an attempt to improve the antimicrobial properties using less amount of citronellol to minimize possible toxic effects that citronellol 20% may have on human skin. PCL 15% αCD 2% citronellol 5% fibers showed significant activity (1–3 log CFU/mL reduction). A further increase in αCD concentration (7%) did not improve the results, which may be related to the preferential binding of citronellol to PCL through hydrophobic interactions and the poor capability of αCD to solubilize citronellol by forming inclusion complexes [58]. αCD may also form poly(pseudo)rotaxanes with PCL increasing the hydrophobicity of the mat [25]. Differently, replacement of αCD by HPβCD (7%) allowed reaching significant antimicrobial activity (1–3 log CFU/mL reduction), and similar to that obtained for PCL 15% αCD 2% citronellol 5% mats.

Cinnamic acid performed differently from carvacrol and citronellol since PCL 15% fibers efficiently encapsulated cinnamic acid up to 20%. PCL 15% fibers prepared with 1, 2, 5 and 10% cinnamic acid did not show antibacterial activity, but those prepared with 20% cinnamic acid displayed significant log CFU/mL reduction (1–3 log CFU/mL reduction; $p < 0.0001$) with respect the other fibers (Fig. 5). Similar bacterial inhibition was recorded for PCL 18% cinnamic acid 30% fibers. The incorporation of αCD at the concentrations of 2% and 7% (*w/v*) did not improve the antibacterial properties. Differently, the incorporation of HPβCD at 7% strongly increased the antibacterial activity (>3 log CFU/mL reduction), reaching a total reduction of CFUs after 24 h contact.

The next step was to explore the synergy that combinations of EOCs may provide to enhance the antimicrobial activity. The antimicrobial activity of fibers containing carvacrol-citronellol, carvacrol-cinnamic acid, and citronellol-cinnamic acid at 1%, 2%, 5%, 10% and 20% (*w/v*) was investigated at PCL concentration of 15%, 18% and 20% (w/v). Note that the percentage of EOC refers to each EOC in the mixture; namely carvacrol-citronellol 5% means that a 5% in each EOC was used to prepare the fibers. Fibers prepared with concentrations lower than 5% (w/v) of each EOC did not show antimicrobial activity, except for PCL 15% carvacrol-citronellol 5% which displayed significantly greater activity (1–3 log CFU/mL reduction; $p < 0.0001$) with respect to other fibers also prepared without HPβCD. Similarly, PCL 18% fibers prepared with citronellol-cinnamic acid mixture at 10–20% exhibited significant antimicrobial activity (1–3 log CFU/mL reduction).

Since the results of the PCL 15–20% fibers with the different mixtures at low concentrations of EOCs did not exhibit relevant antimicrobial activity, HPβCD 7% was incorporated (Fig. 6). All PCL 15% HPβCD 7% fibers prepared with binary and ternary combinations of EOCs showed strong antimicrobial activity (>3 log CFU/mL reduction; $p < 0.0001$ with respect to the other fibers). Indeed, the fibers containing binary combinations of EOCs completely inhibited bacterial growth.

Overall, the three EOCs tested exhibited strong antimicrobial properties when they were loaded into PCL 15% HPβCD 7% fibers, notably surpassing the antimicrobial activity of PCL 15–20% or PCL 15% αCD 2–7% fibers loaded with the same EOC concentrations. Only the PCL 18% fibers that incorporated citronellol 20% alone (not mixed with other EOC) were shown to be equally efficient. Thus, HPβCD improved the antimicrobial properties of the EOCs against *S. aureus* facilitating a log CFU/mL reduction >3 or 4; namely these fibers could kill 99.9% bacteria. This improvement in the antimicrobial activity was mainly due to the high efficiency of the inclusion complex formation of EOCs with HPβCD [59], which resulted in fibers of adequate morphology (avoiding fiber fusion), with a high content in EOCs, and that increased the apparent solubility of the EOCs in the aqueous release medium (PBS), as further investigated in Section 3.4. These two effects (preservation of individualized fibers and hydrosolubilization of EOCs) explain the rapid release and efficient antibiofilm activity of EOCs from the HPβCD-containing fibers. This finding is in good agreement with the decrease in MIC and MBC (up to 8 times) recorded for inclusion complexes of EOCs with different CDs against *S. aureus* and *P. aeruginosa* [60]. Subsequent

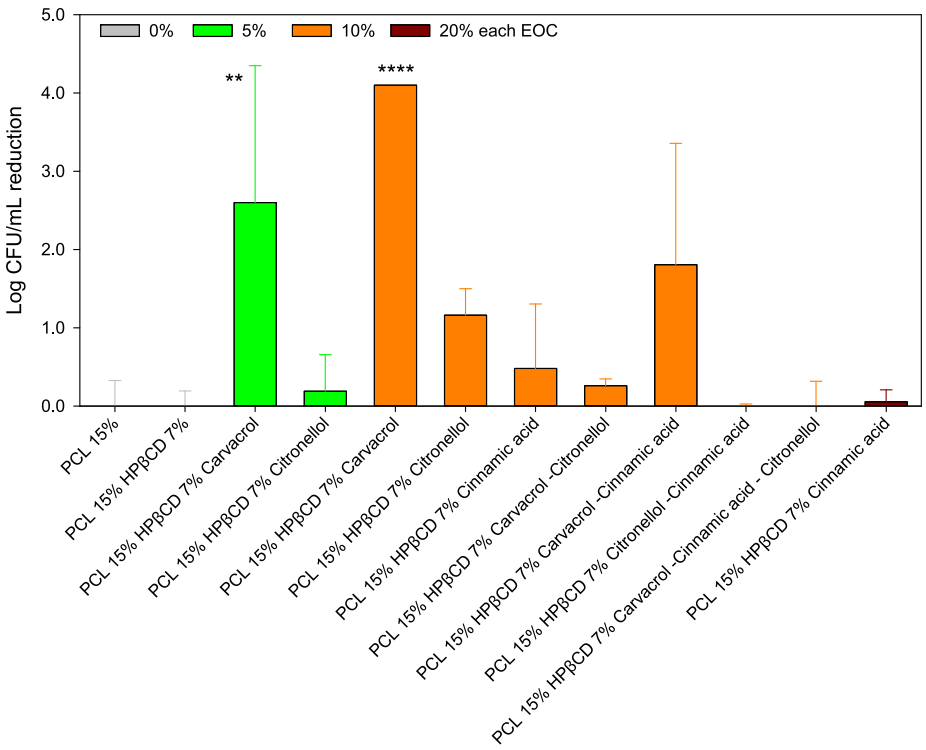

Fig. 7. Preventive action of PCL 15% HP-β-CD 7% fibers loaded with single, binary (1:1) and ternary (1:1:1) mixtures of carvacrol, citronellol and cinnamic acid (from 1 to 20%, as indicated in the legend) against *P. aeruginosa* biofilms, in terms of reduction of culturable cells (log (CFU/mL) reduction) after 24 h contact time. Mean ± standard deviation, $n = 4$, $^{*}p < 0.05$, $^{**}p < 0.005$, $^{***}p < 0.001$ and $^{****}p < 0.0001$.

release tests confirmed the facilitated release of EOCs from PCL 15% HPβCD 7% fibers, as tackled in Section 3.4. The antimicrobial efficacy shown by the EOCs-loaded PCL 15% HPβCD 7% fibers against *S. aureus* were comparable with that of commercial formulations containing silver for treatment of wound infections such as Algicell™, PolyMem® Silver Non-Adhesive Pads, and PolyMem® Silver Shapes [61] that offer an efficacy ≤99.99% of bacterial reduction against *S. aureus*.

3.2.2. *P. aeruginosa* biofilm prevention

The therapeutic arsenal against Gram-negative bacteria, especially *P. aeruginosa*, is scarce and consists mainly of ceftazidime (cephalosporin) and ciprofloxacin (fluoroquinolone) [62]. Resistance against other antibiotics is a major concern. Thus, for *P. aeruginosa* CECT 110 biofilm prevention studies the most efficient fibers against *S. aureus* (CECT 976) were selected, i.e. those made with HPBCD 7% (Fig. 7).

The PCL 15% HPBCD 7% carvacrol 5% fibers caused a significant log CFU/mL reduction (1–3 log CFU/mL reduction; $p < 0.005$). An increase in carvacrol to 10% reduced further the CFUs (4 log CFU/mL reduction; $p < 0.0001$). Differently, citronellol-loaded fibers did not display relevant antimicrobial activity. Poor results were obtained also by the fibers loaded with cinnamic acid. Despite these fibers caused the greatest bacterial inhibition against *S. aureus*, the amount of cinnamic acid that they supplied was not enough to alter *P. aeruginosa* growth. According to literature, cinnamic acid MIC of *P. aeruginosa* is close to 12 mg/mL [57], suggesting that cinnamic acid is not a good candidate for use against this Gram-negative bacterium.

The fibers prepared with binary mixtures of EOCs at 10% (*w/v*) showed minor antimicrobial efficacy against *P. aeruginosa*, quite the opposite to what was observed when tested against *S. aureus*. Only the PCL 15% HPBCD 7% carvacrol-cinnamic acid 10% fibers caused 2 log CFU/mL reduction. Thus, compared to the non-active citronellol and cinnamic acid either alone or mixed together, the presence of carvacrol was required to endow the fibers with antimicrobial efficacy against *P. aeruginosa*. These results agree well with previous reports on the relevant antimicrobial activity of carvacrol against *P. aeruginosa* (MIC 1.18 mg/mL and MBC 2.25 mg/mL) and its capability to inhibit biofilm formation through disruption of the quorum sensing, thus decreasing bacteria pathogenicity [63].

3.3. Biofilm cellular density characterization

To gain a further insight into the *S. aureus* CECT 976 antibiofilm activity of the electrospun fibers, PCL/αCD electrospun mats, epifluorescence microscopy analysis was carried out for a qualitative assessment of the membrane integrity of biofilm cells. Meanwhile, the preventive action of PCL/HPβCD electrospun fibers on *S. aureus* ATCC 25923 and *P. aeruginosa* CECT 110 biofilm set-up was qualitative and quantitative assessed by confocal microscopy.

Regarding epifluorescence microscopy, the control groups showed a high population density of *S. aureus* CECT 976 (Fig. S11A, B and C), with most intact cell membranes (green color) that occupied the greatest area of the field. Meanwhile, few or no cells with membrane damage (red-stained cells) were observed. Collectively, the electrospun mats loaded with EOC (Fig. S11D–L) displayed an increase in the population of cells with membrane damage, highlighting PCL 15% carvacrol-citronellol 5%, PCL 18% citronellol 20%, PCL 15% cinnamic acid 20%, and PCL 18% cinnamic acid 20%. These results are consistent with CFU counting in the section above, showing an equal or more than significant log CFU/mL reduction (1–3 log CFU/mL reduction; $p < 0.05$). Nonetheless, bacterial cells with intact membranes were detected in all fibers despite the high amounts of EOC loaded. In parallel with former section, an improvement in the antibiofilm activity using lower concentrations of EOCs to minimize toxicity in human cells was searched by incorporating HPβCD to the fibers.

In good agreement with Section 3.4 results, the PCL/HPβCD fibers loaded with EOCs exhibited strong antimicrobial activity against sessile cells as revealed by confocal microscopy (Figs. 8 and S12–S26). For each type of fiber, three sets of images were taken: (A) the population of

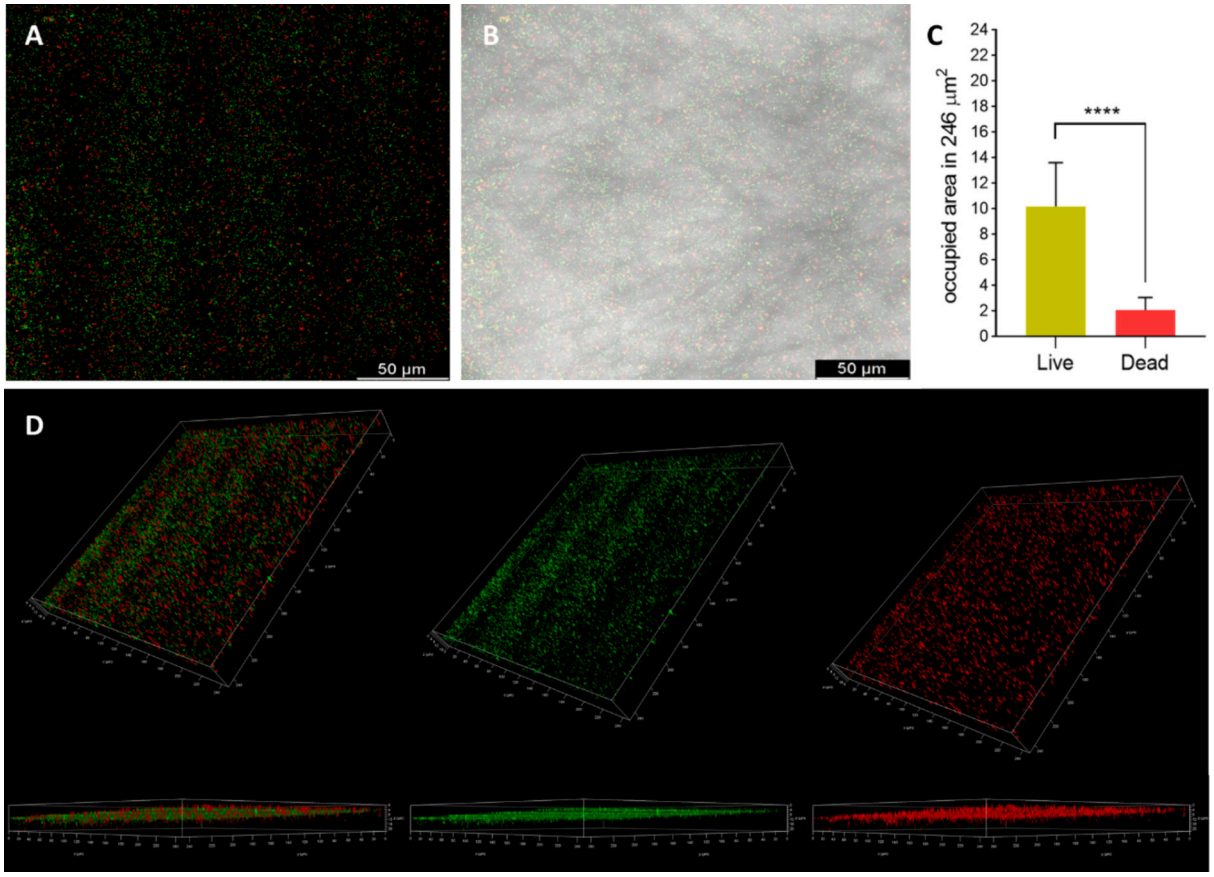

Fig. 8. Confocal microscopy images of *S. aureus* ATCC 25923 biofilms grown on PCL 15% fibers for 24 h under 100 rpm at 37 °C, stained by the Live/dead BacLight bacterial viability kit®. Alive bacterial cells with intact membrane present green fluorescence conferred by SYTO™ 9 dye, while dead bacterial cells present red fluorescence conferred by propidium iodide (PI) dye. (A) Top view of the electrospun mats using the green and red channels; (B) bacterial cells attached on the surface of lengthwise fibers from the electrospun mat; (C) occupied area in 246 μm^2 by intact and dead cells, mean ± standard deviation, $n = 5$; and (D) 3D images of the electrospun mat (length, height, and depth) with the comparison of dead (right) and intact bacteria (center), and both types bacteria (left) on the same plane.

bacterial cells, both alive (intact) and dead, attending only to the emission of fluorescence; (B) the location of the bacterial cells within the fiber; and (D) a three-dimensional representation from which the area occupied by intact/dead bacteria cell layers was calculated (C). Regarding *S. aureus* ATCC 25923, the control PCL 15% electrospun mat (Fig. 8) displayed a high and significant intact population attached to the fibers ($p < 0.0001$) compared to dead bacterial cells, as expected due to the lack of antimicrobial agent. Some bacterial death may be related to the fact that the staining was performed after 24 h of incubation and, therefore, some cells may have entered the death phase. Interestingly, PCL 15% HPβCD 7% fibers without EOCs (Fig. S12) showed some bacterial cells attached to their surface with the same population of intact and dead bacteria, which could be due to a change in surface hydrophobicity, as investigated further in Section 3.5.

PCL 15% HPBCD 7% fibers prepared with carvacrol (Figs. S13 and S14) and cinnamic acid (Figs. S17 and S18) showed a large population of dead bacteria and no population of alive bacteria, obtaining significant differences ($p < 0.0001$) when compared with the controls without EOCs. These results agreed well with the logarithmic reduction > 3 that was obtained in the CFUs. In the case of citronellol-containing fibers (Figs. S15 and S16) both intact and dead bacteria were observed, although with a predominance of dead bacteria ($p < 0.0001$), but the differences were not significant compared to the control.

The fibers prepared with a mixture of EOCs, PCL15% HPBCD 7% carvacrol-citronellol 5% (Fig. S19) and PCL15% HPBCD 7% citronellol-cinnamic acid 10% (Fig. S20) showed good antibiofilm activity, since most *S. aureus* cells were dead (stained red). Differently, the fibers with the mixture of the three EOCs (Fig. S21) had less antimicrobial activity (3 log CFU/mL reduction) and showed an intact population, which can be explained by the relative decrease in the content in carvacrol and cinnamic acid, i.e. the two most efficient EOCs against *S. aureus*.

The antibiofilm properties against *P. aeruginosa* were investigated similarly (Figs. S22–S26). According to the results obtained in Section 3.2.2, only the controls and carvacrol-loaded mats were tested. As expected, PCL 15% (*w/v*) control mats (Fig. S22) showed a large proportion of intact bacteria and some dead bacteria cells. Interestingly, PCL 15% HPβCD 7% control fibers (Fig. S23) displayed less bacteria attached, and the dead population occupied an area similar to that of intact population. This result, also observed when the fibers were exposed to *S. aureus*, suggests that HPβCD interferes with cell adhesion and biofilm development. The capability of HPβCD to alter quorum sensing mechanisms by trapping the communication signals has been previously demonstrated in solution and for gauzes grafted with cyclodextrins [64]. Similarly, the PCL 15% HPβCD 7% fibers can release some HPβCD units to the culture medium and most HPβCD remaining in the fibers can have their cavities available for hosting of quorum sensing signals, as no poly(pseudo)rotaxane formation is expected.

PCL 15% HPβCD 7% loaded with carvacrol at 5%–10% (w/v) (Figs. S24 and S25) evidenced that most area was occupied by dead bacteria. No intact bacteria were detected. Moreover, these electrospun mats displayed significant differences ($p < 0.05$) with respect to the control. The area occupied by dead bacteria was lower in the PCL 15% HPβCD 7% carvacrol-cinnamic acid 10% mats (Fig. S26), but still their capability to kill *P. aeruginosa* was remarkable. Quenching of the quorum sensing mechanism of communication among bacteria has been demonstrated as an efficient way of haltering *P. aeruginosa* biofilm

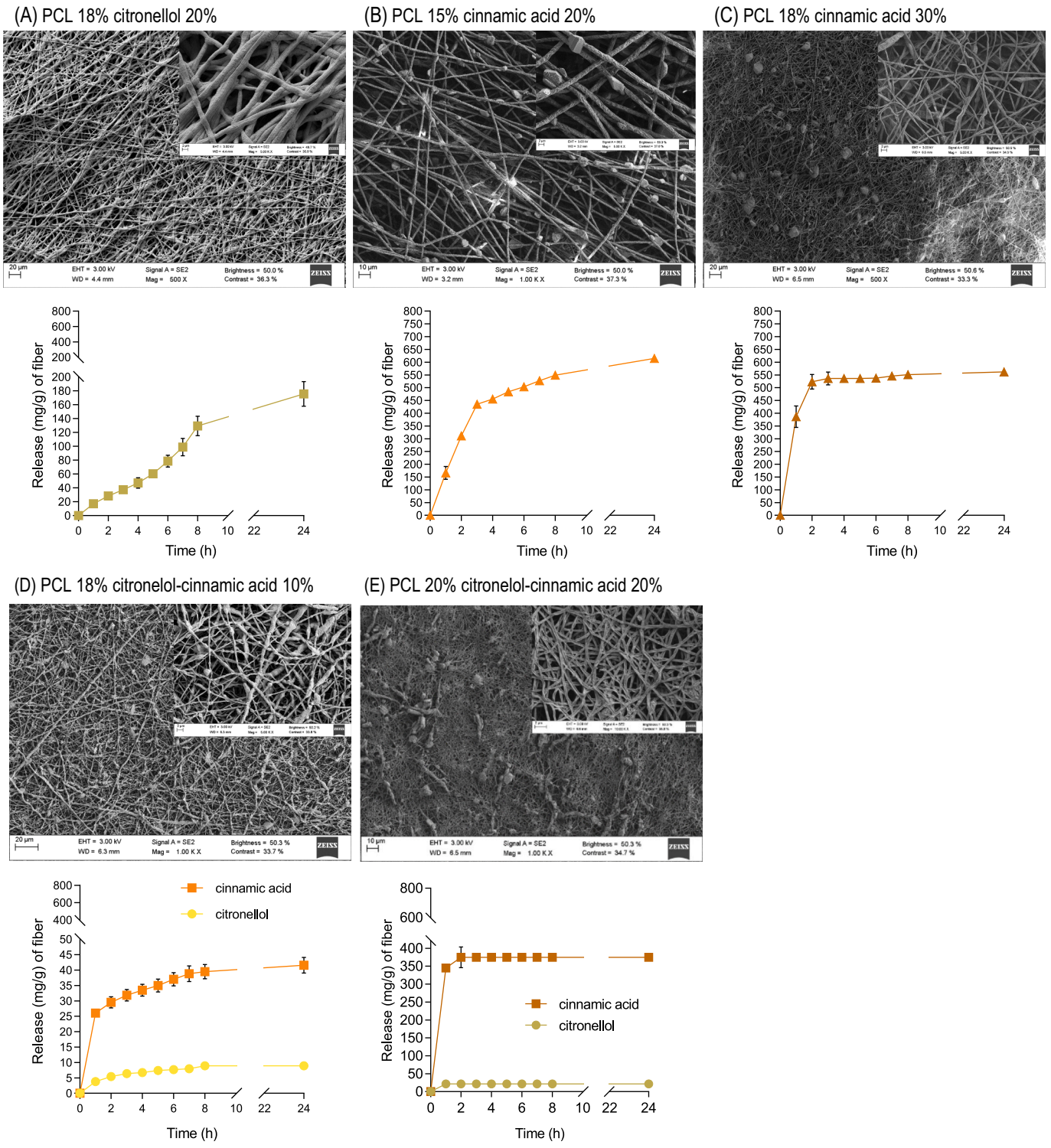

Fig. 9. FESEM images with 500× and 5000× magnification with scale bar 20 μm and 2 μm, respectively, and, below, the cumulative amounts released of EOCs in PBS (pH 7.4), under 100 rpm and 37 °C for 24 h ($n = 3$) recorded for (A) PCL 18% citronellol 20%, (B) PCL 15% cinnamic acid 20%, (C) PCL 18% cinnamic acid 30%, (D) PCL 18% citronelol-cinnamic acid 10%, and (E) PCL 20% citronelol-cinnamic acid 20% electrospun mats.

formation [65], and both HPβCD and carvacrol in separate have demonstrated capability to inhibit quorum sensing through different mechanisms [63,66]. Such a capability explains the successful results recorded for electrospun mats that combine HPβCD and carvacrol.

3.4. Structural characterization and release pattern of the antibiofilm fibers

Fibers exhibiting antibiofilm activity were investigated in more detail regarding morphology (FESEM images), crystallinity (DSC) and release profiles of the EOC/s in PBS (pH 7.4) at 37 °C. It should be noted that pristine carvacrol and citronellol are liquid at room temperature

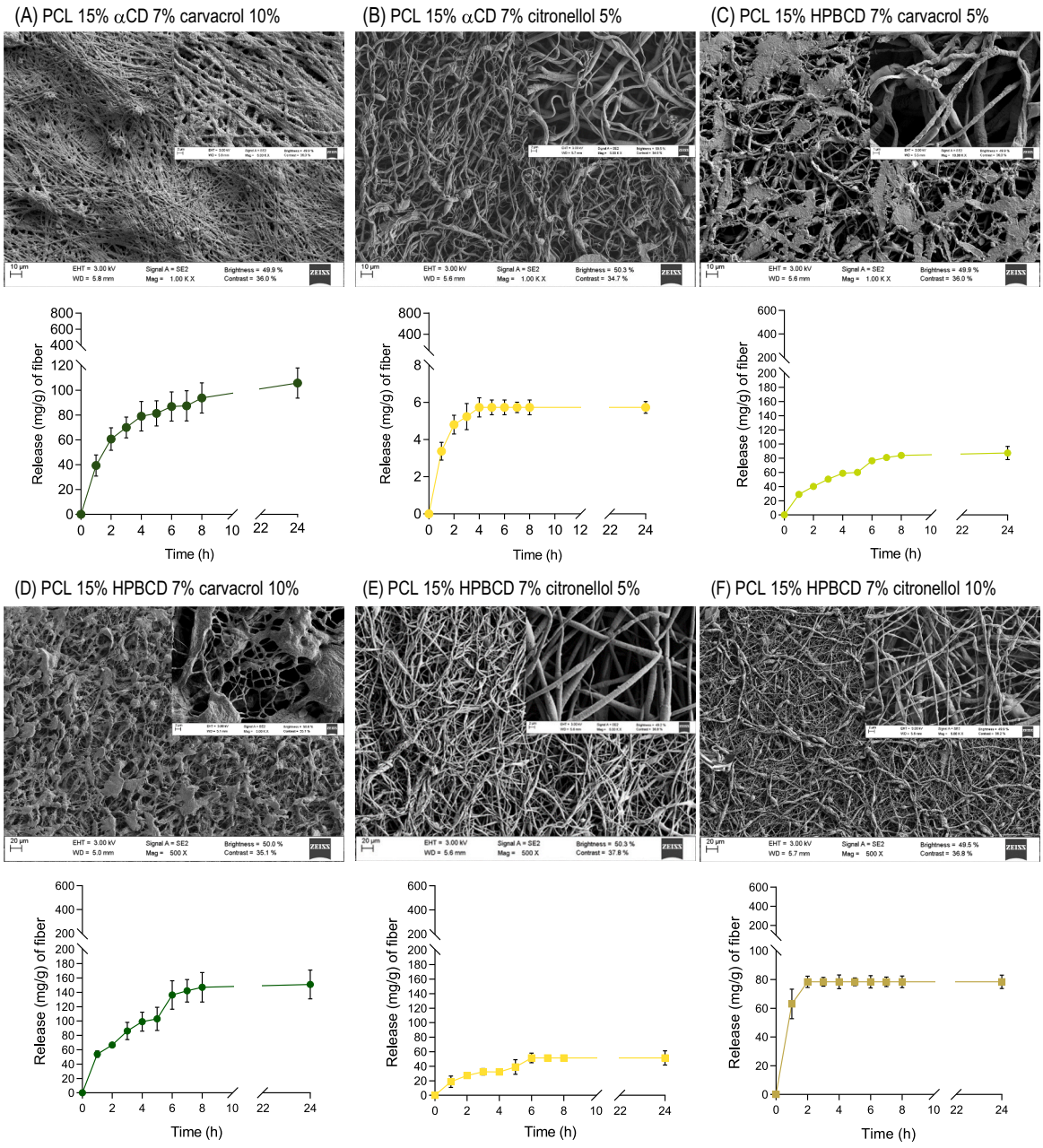

Fig. 10. FESEM images with 500× and 5000× magnification with scale bar 20 μm and 2 μm, respectively, and, below, the cumulative amounts released of EOCs in PBS (pH 7.4), under 100 rpm and 37 °C for 24 h ($n = 3$) recorded for (A) PCL 15% αCD 7% carvacrol 10%, (B) PCL 15% αCD 7% citronellol 5%, (C) PCL 15% HPβCD 7% carvacrol 5%, (D) PCL 15% HPβCD 7% carvacrol 10%, (E) PCL 15% HPβCD 7% citronellol 5%, and (F) PCL 15% HPβCD 7% citronellol 10% electrospun mats.

while cinnamic acid is formed by crystalline particles that melt at 135 °C (Fig. S27).

Three fibers prepared with PCL solely were first characterized: PCL 18% citronellol 20%, PCL 15% cinnamic acid 20%, and PCL 18% cinnamic acid 30%. These fibers had in common that they were loaded with the maximum content in EOC that the fibers allowed. PCL 18% citronellol 20% fibers (1660 ± 480 nm) maintained the cylindrical shape without beads despite the high amount of citronellol that was incorporated (Fig. 9A). This electrospun mat showed sustained release of citronellol, with 170 mg released per gram of fiber at 24 h. Such a slow release, but still sufficient to provide antibiofilm levels (see Fig. 4), may be related to the moderate solubility of citronellol in water (200 mg/L) and logP 3.2 (PubChem database) and to an efficient encapsulation inside the fibers. No relevant changes were recorded in the DSC scans of these fibers compared to raw PCL (Fig. S27) and PCL solely fibers (Fig. S28), showing similar melting temperature (57 °C) and enthalpy (59.7 J/g).

PCL fibers saturated with cinnamic acid, i.e. PCL 15% cinnamic acid 20% (1730 ± 160 nm; Fig. 9B) and PCL 18% cinnamic acid 30% (610 ± 240 nm; Fig. 9C), had homogeneous, smooth and continuous shape, including cinnamic acid aggregates attached lengthwise the fiber. These two electrospun mats released rapidly a first fraction of the amount loaded (310 mg/g and 510 mg/g, respectively) in the first 2–3 h. This burst release is related to cinnamic acid particles crystallized on the surface of the fibers, as confirmed by the DSC characteristic peaks of cinnamic acid melting (122–126 °C) (Fig. S28) although they appeared at slightly lower temperature than for the raw EOC (135 °C). The melting enthalpy values revealed that 55% and 64% cinnamic acid remained as crystalline particles on the PCL 15% cinnamic acid 20% and PCL 18% cinnamic acid 30% fibers, respectively. The subsequent slower

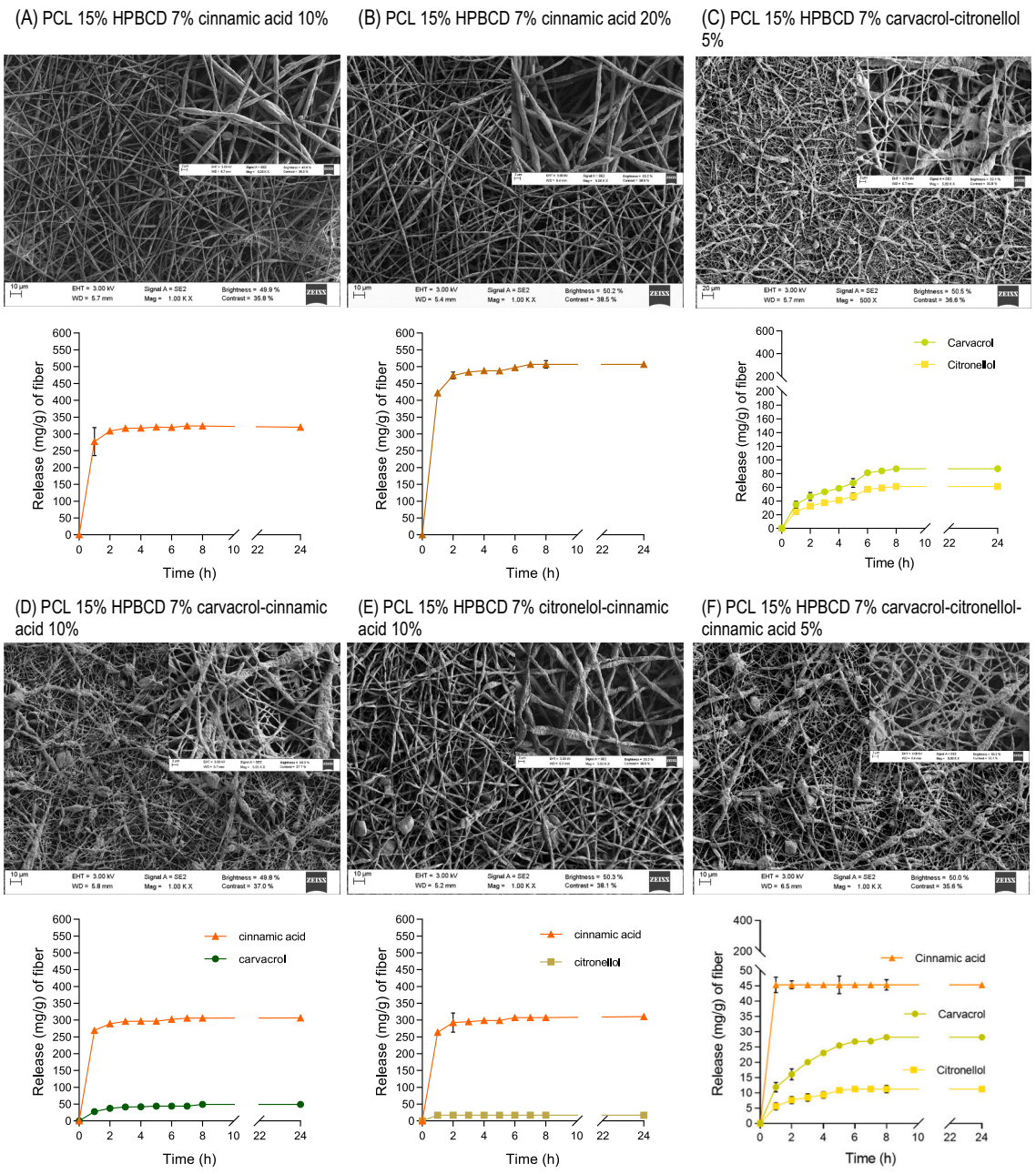

Fig. 11. FESEM images with 500× and 5000× magnification with scale bar 20 μm and 2 μm, respectively, and, below, the cumulative amounts released of EOCs in PBS (pH 7.4), under 100 rpm and 37 °C for 24 h ($n = 3$) recorded for (A) PCL 15% HPβCD 7% cinnamic acid 10%, (B) PCL 15% HPβCD 7% cinnamic acid 20%, (C) PCL 15% HPβCD 7% carvacrol-citronellol 5%, (D) PCL 15% HPβCD 7% carvacrol-cinnamic acid 10%, (E) PCL 15% HPβCD 7% citronellol-cinnamic acid 10%, and (F) PCL 15% HPβCD 7% carvacrol-citronellol-cinnamic acid 5% electrospun mats.

release step could correspond to cinnamic acid encapsulated inside the fibers. After 24 h in the release medium, PCL 15% cinnamic acid 20% released 650 mg/g, and PCL 18% cinnamic acid 30% released 530 mg/g, which corresponded to ca. 100% loaded. As depicted in Fig. 5, the release of such high amounts of cinnamic acid efficiently prevented *S. aureus* biofilm formation.

PCL fibers prepared with mixtures of citronellol and cinnamic acid were also evaluated. The PCL 18% citronellol-cinnamic acid 10% fibers had cylindric shape but with some aggregates lengthwise of the fibers (fibers size 410 ± 140 nm; Fig. 9D) that resembled the cinnamic acid crystals. Interestingly, PCL 20% citronellol-cinnamic acid 20% mat was formed by more homogeneous fibers without beads, but they lost the cylindrical shape and adopted a ribbon-like structure due to the increase in the EOCs:polymer ratio (fibers size 400 ± 40 nm; Fig. 9E). These dually loaded fibers also showed a very rapid release of cinnamic acid and slow release of citronellol, in good agreement with the results recorded for the fibers prepared with only one EOC. As explained above, fast dissolution of cinnamic acid correlated well with the presence of the crystals of this EOC on the mat surface. However, interestingly, the fibers co-loaded with citronellol and cinnamic acid evidenced lower melting temperature and enthalpy of cinnamic acid (Fig. S28) than those of raw cinnamic acid, which suggests that cinnamic acid can partially dissolve in citronellol and thus less crystals are formed. Concerning to citronellol release profile, both mats released similar amounts, 7–8 mg/g, despite PCL 20% citronellol-cinnamic acid 20% were prepared with double concentration of citronellol than PCL 18% citronellol-cinnamic acid 10% fibers. Citronellol (200 mg/L aq. solubility; log P 3.1) is more hydrophobic than cinnamic acid (500 mg/L aq. solubility; log P

2.2; PubChem database), being more compatible with PCL. Citronellol may establish hydrophobic interactions, dipole-dipole or van der Waals forces with PCL, more favourably than cinnamic acid, which may help citronellol to remain inside the PCL fiber matrix. Differently, migration to the surface of PCL matrices has already been described for polar active ingredients, similar to cinnamic acid, which facilitates drug release and, in this case, the antibiofilm activity [67].

Regarding the fibers containing cyclodextrins, PCL 15% αCD 7% carvacrol 10% mats were formed by homogeneous, continuous fibers without beads (fibers diameter 1040 ± 200 nm; Fig. 10A). Although the fibers were partially fused together, the mat was still porous and efficiently released carvacrol to the aqueous medium. The addition of αCD improved the loading of high amounts carvacrol and controlled the release for 24 h. PCL 15% αCD 2% citronellol 5% mat, which also exhibited antimicrobial properties, was made of continuous fibers (720 ± 420 nm; Fig. 10B). This mat showed a burst release in the first 4 h with 5 mg citronellol released per gram of fiber, which corresponded to a 22% of the initial content. These two mats showed the characteristic thermal events of PCL, but the fibers containing carvacrol had a second endothermic peak at 67.39 °C (Fig. S29). This unexpected peak, which also appeared in PCL 15% HPβCD 7% carvacrol 10% mats, may suggest that carvacrol forms cocrystals with other components of the fibers. It has been reported that carvacrol itself crystallizes at −20 °C and melts between 0 and 3.5 °C [68] and that readily forms cocrystals with a variety of molecules [69]. The crystallization of carvacrol was not seen in the DSC scans of the fibers, mainly because the crystallization process is quite slow and the sample requires time to trigger crystal formation [68]. To the best of our knowledge, *co*-crystallization of carvacrol with a polymer has only been reported so far for polystyrene films processed in organic solvents like those used to prepare our fibers [70]. These authors found that such a co-crystallization decreased the desorption rate of carvacrol and provided prolonged antimicrobial effects.

Replacement of HPβCD by αCD did not prevent completely the fusion of fibers containing carvacrol. PCL 15% HPβCD 7% fibers prepared with carvacrol 5% (960 ± 550 nm; Fig. 10C) and carvacrol 10% (520 ± 270 nm; Fig. 10D) were continuous, but aggregation of fibers was observed. Both mats released carvacrol gradually during 8 h, and the amounts released at that time were 80 mg/g and 140 mg/g, respectively, which corresponded to 43.2% and 44.9% loaded, and according to the antibiofilm results (Fig. 3) sufficient to inhibit *S. aureus* growth. Only the mat with the highest content in carvacrol showed, in addition to the PCL melting peak, an additional endothermic event which might be related to co-crystallization (Fig. S29).

PCL 15% HPBCD 7% citronellol 5% fibers were continuous and without beads (520 ± 270 nm; Fig. 10E). Doubling the content in citronellol caused some beads to appear in the fibers (530 ± 200 nm; Fig. 10F) but fusion was not observed. The small diameter of citronellol-loaded fibers could be due to a decrease in the dielectric constant of the solutions caused by the EOC. These results agreed well with other fibers loaded with citronellol. These fibers released 40 mg/g and 80 mg/g, respectively, which corresponded to 21.6% and 25.6% loaded. The slower release rate of citronellol compared to carvacrol from fibers of the same composition can be related to lower solubility in aqueous medium of citronellol (200 mg/L) compared to carvacrol (1.2 g/L). Thus, these citronellol mats exhibited slightly lower antimicrobial activity against *S. aureus* and higher MBC (citronellol 1 mg/mL; carvacrol 0.8 mg/mL). These two mats only showed the characteristic thermal events of PCL (Fig. S30).

In the case of cinnamic acid-loaded fibers, the addition of HPβCD favored the encapsulation of cinnamic acid into the PCL fibers and reduced to a minimum the formation of EOC crystals on the mats surface, as confirmed by the marked decrease in the melting enthalpy of the cinnamic acid (Fig. S30). These mats showed the characteristic melting peak of cinnamic acid at 107–118 °C but the enthalpy values reflected that only 20–23% cinnamic acid remaining as free crystalline particles. PCL 15% HPBCD 7% fibers prepared with cinnamic acid 10% (1130 ± 340 nm; Fig. 11A) or cinnamic acid 20% (1220 ± 300 nm; Fig. 11B) displayed a huge burst release in first hour, releasing 300 mg/g and 500 mg/g, respectively, which corresponded to approx. 100% loaded. Therefore, the inclusion complex formation of cinnamic acid with HPβCD prevented cinnamic acid crystallization and notably accelerated the dissolution, which explains the higher antimicrobial activity of these fibers compared to those lacking HPβCD (PCL solely and PCL-αCD fibers).

Results obtained for electrospun mats loaded with binary and tertiary mixtures of EOCs are summarized in Fig. 11C–F. PCL 15% HPβCD 7% carvacrol-citronellol 5% displayed continuous fibers without beads but presented a variety of sizes (520 ± 270 nm) due to an irregular encapsulation by an excess of EOCs (Fig. 11C). HPβCD prevented the complete fusion of the fibers recorded for PCL 15% fibers with these two EOCs. Moreover, the mixture of two EOCs displayed important advantages with positive synergism; PCL 15% HPβCD 7% carvacrol-citronellol 5% released amounts of EOCs similar to those released by fibers containing carvacrol (Fig. 10C) and citronellol (Fig. 10E) in separate: 80 mg/g carvacrol and 50 mg/g citronellol at same time 24 h. These values corresponded to 51.3 and 32.1% loaded, respectively, which means that the fibers loaded with a binary mixture released the EOCs at the same rate or even faster than the single loaded fibers.

Similar results were obtained with the carvacrol and cinnamic acid mixture showing a positive synergism. PCL 15% HPβCD 7% carvacrol-cinnamic acid 10% mats displayed continuous fibers (740 ± 470 nm) and without beads but exhibit thickening lengthwise the fiber and some characteristic cinnamic aggregates, which can be due to a preferential interaction of carvacrol with HPβCD, triggering the migration of cinnamic acid towards the fibers surface. Nevertheless, the melting enthalpy of cinnamic acid peak was relatively small suggesting amorphization in these fibers (Fig. S30). These fibers released 50 mg/g of carvacrol, which was less than the amount released by single carvacrol 5% mat. Differently, cinnamic acid reached 100% release, which explains their remarkable antibiofilm activity (Fig. 6).

Similarly, PCL 15% HPBCD 7% citronellol-cinnamic acid 10% were formed by continuous fibers (1280 ± 600 nm; Fig. 11E) with some cinnamic acid crystals on the surface and showed a fast and complete release of cinnamic acid. Instead, less amount of citronellol, 20 mg/g, was released.

Fibers prepared with a mixture of the three EOCs, PCL 15% HPBCD 7% carvacrol-citronellol-cinnamic acid 5% were continuous, homogeneous, without beads (560 ± 190 nm) but with thickening lengthwise due to an improper encapsulation of hydrophobic carvacrol and citronellol and some characteristic cinnamic acid aggregates. The fibers released the three EOCs at different rates as a function of their polarity, as clearly depicted in Fig. 11F. Such release pattern was highly efficient to inhibit *S. aureus* biofilm (Fig. 6), but not *P. aeruginosa* growth (Fig. 7).

It should be noted that the PCL fibers did not significantly swell or erode in contact with the release medium for 24 h, which facilitates their application and removal from the wound bed if needed.

3.5. Surface polarity

The hydrophobic, polar, and apolar components of the surface tension of the mats prepared with and without EOCs are summarized in Table S2 and S3 in Supplementary Material.

The apolar and polar surface properties of the electrospun fibers were determined by Lifshitz-van der Waals component γ^{LW} and the Lewis acid-base component γ^{AB}, respectively. The values of the nonpolar component γ^{LW} were close to 40 mJ/m^2, which is a common value for organic polymers and biopolymers [48]. PCL electrospun mat had a value of 40.68 mJ/m^2. Indeed, the values of γ^{LW} of the electrospun mats hardly changed with the incorporation of EOCs because the main component was PCL. The polar surface tension component, γ^{AB}, of the fibers had a value of 0 for PCL and PCL/αCD fibers. These kinds of fibers

Table 1
Mechanical properties of fibers prepared with different contents in EOCs. Mean values ($n = 3$; standard deviations below 10% in all cases).

Fiber type	Young's modulus (MPa)	Tensile strength (MPa)	Elongation at break (%)
PCL 15%	367.36	80.72	97.43
PCL 15% αCD 2%	5291.70	1274.99	85.34
PCL 15% αCD 7%	167.79	55.93	92.05
PCL 20% citronellol 20%	32.20	4.65	97.56
PCL 18% cinnamic acid 20%	9.54	0.44	6.23
PCL 20% cinnamic acid 30%	2.62	1.64	72.98
PCL 18% citronellol-cinnamic acid 10%	4.27	0.19	0.2
PCL 20% citronellol-cinnamic acid 20%	3.74	0.12	4.89
PCL 15% αCD 2% carvacrol 10%	151.87	20.53	114.63
PCL 15% αCD 2% citronellol 5%	88.48	10.63	197.96
PCL 15% HPβCD7%	222.42	37.48	198.00
PCL 15% HPβCD7% carvacrol 5%	56.24	16.49	198.00
PCL 15% HPβCD7% carvacrol 10%	7850.80	354.72	45.67
PCL 15% HPβCD7% citronellol 5%	19.57	1.58	117.09
PCL 15% HPβCD7% citronellol 10%	0.70	0.26	42.51
PCL 15% HPβCD7% cinnamic acid 10%	16.62	3.56	22.97
PCL 15% HPβCD7% cinnamic acid 20%	83.99	3.78	5.60
PCL 15% HPβCD7% carvacrol-citronellol 5%	19.21	6.11	109.77
PCL 15% HPβCD7% carvacrol-cinnamic acid 10%	157.13	1.26	0.49
PCL 15% HPβCD7% citronellol-cinnamic acid 10%	5.98	0.06	4.74
PCL 15% HPβCD7% carvacrol-citronellol-cinnamic acid 5%	378.52	0.61	6.65

displayed 0 proton acceptor or electron donor γ^-. The γ^{AB} values were calculated applying Eq. (3) [48]:

$$\gamma^{AB} = 2\sqrt{\gamma^+\gamma^-} \quad (3)$$

where γ^- is the proton acceptor or electron donor component and γ^+ the electron acceptor component. The values of γ^+ increased slightly with the addition of EOCs to the fibers because they have electron-accepting functional groups. Cinnamic acid has a COOH acid group in its structure, while carvacrol and citronellol have OH groups. These later groups are strong electron donors and decreased the γ^+ values. The same phenomenon occurred for fibers with cyclodextrins which also had lower γ^+ values than fibers with only PCL mainly due to their OH groups. Meanwhile, some PCL/HPβCD fibers showed opposite behavior, $\gamma^+ > \gamma^-$, being electron donor due to the structural differences between αCD and HPβCD.

PCL and PCL αCD fibers showed $\Delta G^{TOT} < 0$ mJ/m^2, indicating the hydrophobic character of these fibers, which could be increased due to poly(pseudo)rotaxane formation [71]. Differently, some PCL/HPβCD fibers displayed a $\Delta G^{TOT} > 0$ mJ/m^2 indicating hydrophilic character. This change of hydrophobicity could be relevant in terms of bacteria adhesion since the adhesion is hindered when $\Delta G^{TOT} > 0$ mJ/m^2, while $\Delta G^{TOT} < 0$ mJ/m^2 may favor the adhesion [72].

Overall, the fibers tested in this study had hydrophobic surface, as expected for PCL materials, except for some fibers prepared with HPβCD. The incorporation of EOCs attenuated the hydrophobicity, reducing the ΔG^{TOT}. This reduction could be due to the presence of free EOC on the surface of the fibers. Also, the formation of EOC-cyclodextrin inclusion complexes in the vials before the electrospinning process can attenuate the poly(pseudo)rotaxane formation with PCL.

Table 2
Antioxidant properties of EOCs eluted from PCL 15% HPβCD7% fibers after soaking in PBS at 37 °C and 100 rpm during 24 h. ****p < 0.0001; statistically significant difference with non-loaded PCL 15% HPβCD 7% fibers.

Fiber type	DPPH scavenging effect (%)	DPPH (μg/ml)
PCL 15% HPβCD7%	5.72 ± 2.85	30.52 ± 0.16
PCL 15% HPβCD7% carvacrol 5%	22.11 ± 2.64 ****	25.04 ± 0.93
PCL 15% HPβCD7% carvacrol 10%	27.20 ± 0.95 ****	23.33 ± 0.30
PCL 15% HPβCD7% citronellol 5%	9.37 ± 3.22	29.32 ± 1.63
PCL 15% HPβCD7% citronellol 10%	7.27 ± 2.47	30.00 ± 0.23
PCL 15% HPβCD7% cinnamic acid 10%	4.84 ± 5.11	30.81 ± 1.02
PCL 15% HPβCD7% cinnamic acid 20%	11.99 ± 2.77	28.42 ± 0.19
PCL 15% HPβCD7% carvacrol-citronellol 5%	27.62 ± 2.52 ****	23.50 ± 0.49
PCL 15% HPβCD7% carvacrol-cinnamic acid 10%	55.30 ± 4.50 ****	13.90 ± 1.50
PCL 15% HPβCD7% citronellol-cinnamic acid 10%	4.63 ± 3.57	30.89 ± 0.57
PCL 15% HPβCD7% carvacrol-citronellol-cinnamic acid 5%	29.99 ± 2.21 ****	22.38 ± 0.20

3.6. Mechanical properties of electrospun mats

The tensile properties of PCL, PCL/αCD and PCL/HPβCD mats with different concentration of EOC were characterized in terms of Young's modulus, tensile strength and elongation at break (Table 1; Fig. S31). Addition of EOC to PCL solely fibers caused a decrease in Young's modulus and the fibers became brittle, suggesting that intercalation of EOC disrupted the intermolecular bonding among PCL chains, which may also explain the fast release from fibers prepared with 20% EOCs and the antibiofilm activity of some of them. Relevantly, PCL 15% αCD 2% control mat had remarkably higher Young's modulus and tensile strength, conforming the reinforcement of the fibers when poly(pseudo) rotaxanes are formed, in good agreement with previous results [25]. However, an excess in αCD (7%) restored the balance of intermolecular forces and the fibers performed similarly to PCL 15% mats. As expected, incorporation of EOCs, although weakly interacting with αCD compared to HPβCD [73], weakened the mechanical properties of the fibers as EOCs can attenuate poly(pseudo)rotaxane formation. In the case of PCL/HPβCD mats the results were similar to those recorded for PCL mats, with the exception of PCL 15% HPβCD7% carvacrol 10%, which were more rigid. Regarding the fibers prepared with the three EOCs (Table 1, last row), they were very brittle and broke easily when handled.

3.7. Antioxidant activity

In addition to antimicrobial properties, EOCs are commonly characterized by antioxidant activity, exerting synergic outcomes during wound healing [15,33]. First, the antioxidant properties of each free EOC was tested using concentrations in the 0.01–15.0 mg/mL in EtOH: PBS (50:50) medium. At the highest concentration, the DPPH scavenging capability ranked in the order cinnamic acid (50%) > carvacrol (30%) > citronellol (10%). Interestingly, carvacrol displayed 10% DPPH scavenging effect at 0.01 mg/mL (the lowest concentration tested), while cinnamic acid needed 0.94 mg/mL to achieve 10% DPPH scavenging effect.

In good agreement with the results obtained for free EOCs, fibers

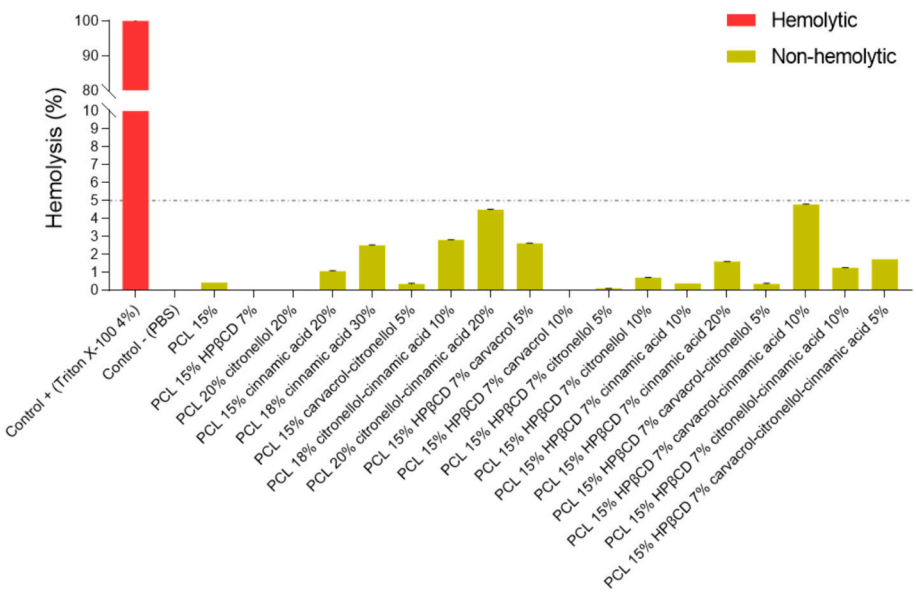

Fig. 12. Hemolysis recorded for the fibers loaded with different EOCs after 1 h incubation. Hemocompatibility threshold (5% hemolysis) is shown as a dotted line.

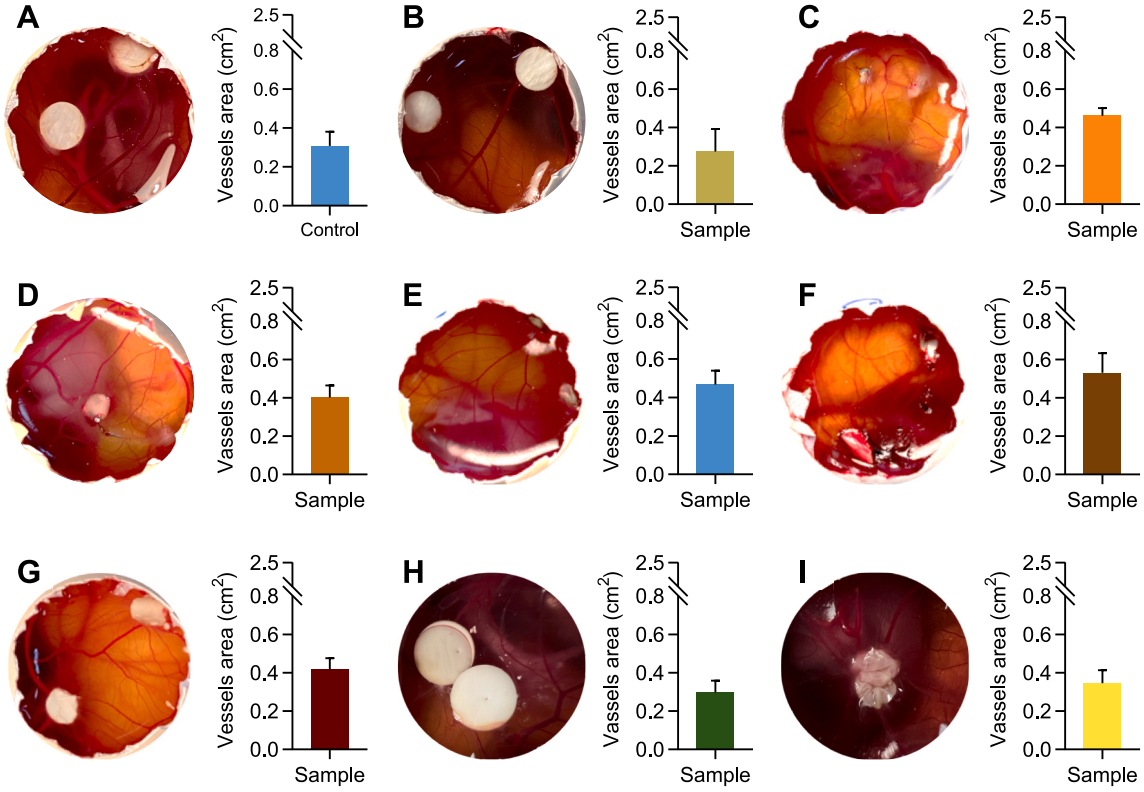

Fig. 13. CAM pictures and vascularization of A) PCL 15% (control), B) PCL 20% citronellol 20%, C) PCL 15% cinnamic acid 20%, D) PCL 18% cinnamic acid 30%, E) PCL 15% carvacrol-citronellol 5%, F) PCL 18% citronellol-cinnamic acid 10%, G) PCL 20% citronellol-cinnamic acid 20%, H) PCL 15% αCD 7% carvacrol 10%, and I) PCL 15% αCD 7% citronellol 5% mats. Data are presented as the mean ± standard deviation, $n = 4$.

loaded with carvacrol surpassed 20% DPPH scavenging after 24 h contact, showing statistical differences ($p < 0.0001$) with respect to the PCL 15% HPβCD 7% (control) mats (Table 2). The electrospun mat that displayed the highest scavenging effect (55.30 ± 4.50%) was PCL 15% HPβCD 7% carvacrol-cinnamic acid 10% owing to the high antioxidant activity of carvacrol and cinnamic acid, indicating a positive synergic effect since their antioxidant activity was twofold higher than that of fibers with same concentration of carvacrol. The second more efficient mats were those of PCL 15% HPβCD 7% carvacrol-citronellol-cinnamic acid 5% and PCL 15% HPβCD 7% carvacrol-citronellol 5%, which had 29.99 ± 2.21% and 27.62 ± 2.52% scavenging capability, respectively (Table 2).

Cinnamic acid electrospun mats displayed a notably DPPH scavenging only when the content in this EOC reached 20%, while citronellol-loaded fibers were the ones with the lowest antioxidant capability.

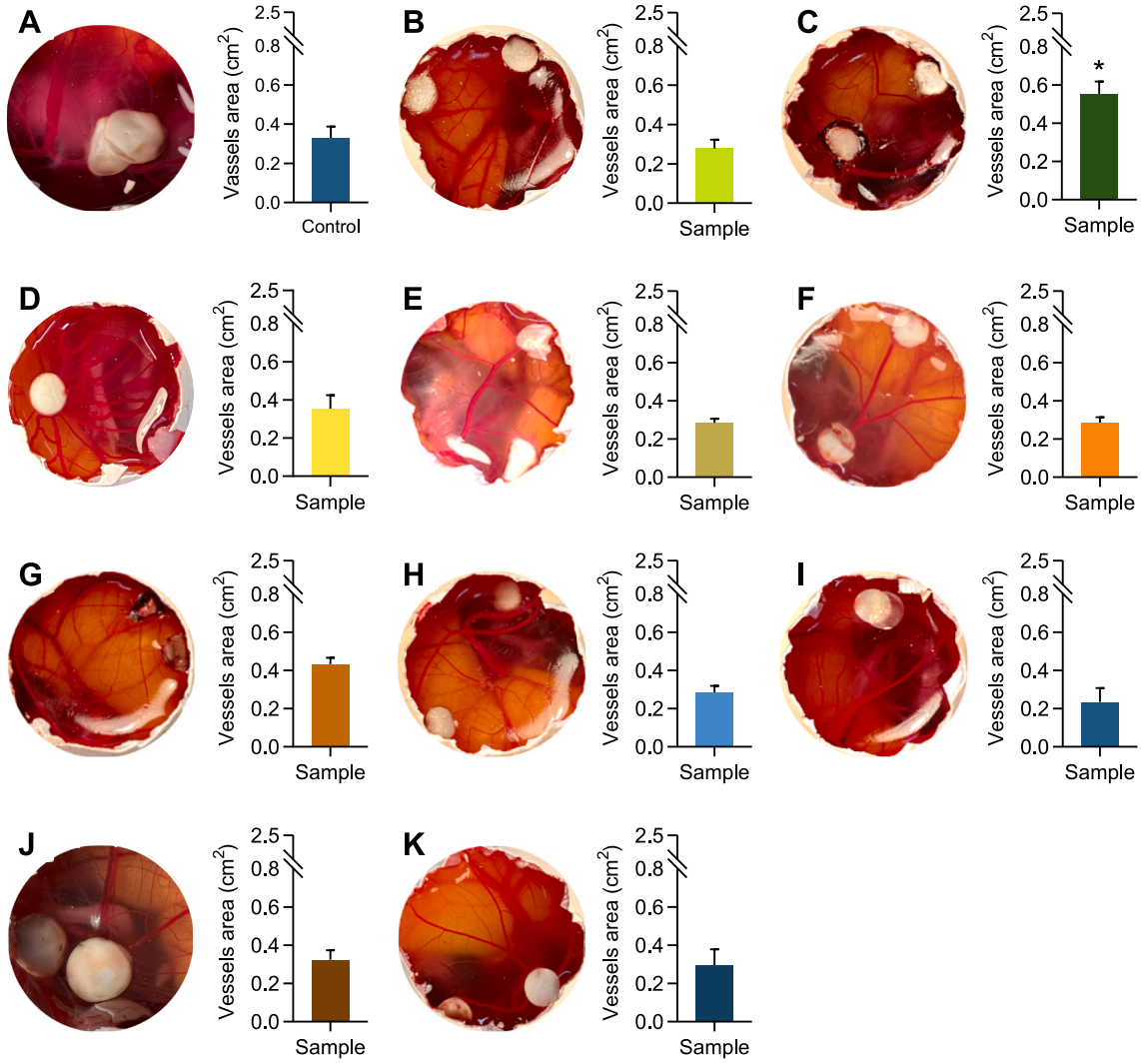

Fig. 14. CAM pictures and vascularization of A) PCL 15% HPβCD 7% (Control), B) PCL 15% HPβCD 7% carvacrol 5%, C) PCL 15% HPβCD 7% carvacrol 10%, D) PCL 15% HPβCD 7% citronellol 5%, E) PCL 15% HPβCD 7% citronellol 10%, F) PCL 15% HPβCD 7% cinnamic acid 10%, G) PCL 15% HPβCD 7% cinnamic acid 10%, H) PCL 15% HPβCD 7% carvacrol-citronellol 5%, I) PCL 15% HPβCD 7% carvacrol-carvacrol 10%, J) PCL 15% HPβCD 7% citronellol-cinnamic acid 10%, and K) PCL 15% HPβCD 7% carvacrol-citronellol-cinnamic acid 5% mats. Data are presented as the mean ± standard deviation, n = 4, $*p < 0.05$.

3.8. Hemolysis test

The fibers with the highest antimicrobial activity were also evaluated in terms of hemocompatibility as a preliminary screening of biocompatibility. All fibers tested showed excellent blood compatibility with hemolysis percentages lower than 5% even for the fibers containing the highest concentrations in binary mixtures of EOCs (Fig. 12).

3.9. In ovo tissue integration and angiogenesis evaluation

Finally, a CAM test was carried out to gain a further insight into biocompatibility, toxicity, angiogenesis response, and tissue integration of the developed mats. The CAM test has been proved to be a good alternative method to in vivo studies for formulations intended to be in contact with skin and mucosa, facilitating the reducing, replacement and refining of animal models [74,75]. The CAM test is more available and cost effective, and allows complete accessibility to the circulatory system [53]. The CAM is a membrane sensitive to toxic agents and in few minutes can develop irritation signs such haemorrhage, vascular lysis or coagulation.

In our case, the fibers were in contact with the CAM for 5 days and no signs of hemolysis or toxicity were recorded. The integration and vascularization of the fibers are shown in Figs. 13 and 14. All fibers had an integration score of 2 out of 3, showing good interaction with the surface that was in contact with the CAM. In general, vascularization was not affected, indicating that the amounts of EOC released from the fibers did not trigger angiogenic effects. Some authors reported that cinnamic acid and its derivatives have angiogenic capacities due to the regulation of VEGF and Flk-1/KDR expression [76]. Indeed, in the case of the fibers prepared without cyclodextrins, only those that incorporated cinnamic acid slightly increased the angiogenesis, but the change was not statistically different compared to the control (Fig. 13C, D, F).

When quantifying the area occupied by the blood vessels, fibers prepared with cyclodextrins performed similarly to PCL solely fibers, except for those prepared with the highest amount in carvacrol. PCL 15% HPβCD 7% carvacrol 10% exhibited angiogenic activity showing a significant increase compared to the controls ($p < 0.05$). Some authors have reported that carvacrol promotes angiogenesis at low concentrations by increasing VEGF levels and the formation of tubular arrays [77].

Overall, all the fibers tested showed good biocompatibility and no toxic effects despite the high concentration of EOCs with which they were loaded. In addition, these fibers had good integration scores, which may facilitate wound healing, also aided by angiogenesis in the case of those prepared with cinnamic acid and carvacrol.

4. Conclusions

Electrospun fibers loaded with single and combined EOCs were successfully prepared using PCL at 15–22% (*w/v*) as structural polymer and αCD 2–7% (w/v) or HPβCD 7% (w/v) as encapsulating agent. Three types of EOCs of different physicochemical properties were investigated to demonstrate the versatility of the approach.

αCD promoted the formation of poly(pseudo)rotaxanes with PCL, reinforcing the mechanical properties of the fibers, but did not significantly contribute to facilitating the integration of the EOCs within the fibers. Differently, the greater capacity of HPβCD to form inclusion complexes with EOCs, and not form poly(pseudo)rotaxanes with PCL, facilitated the homogeneous incorporation of the EOCs. More specifically, HPβCD prevented from fusion of the fibers, attenuated the crystallization of cinnamic acid on the fibers surface, and provided an adequate balance of high loading and sufficiently rapid release of EOCs to obtain strong antimicrobial activity. Binary and ternary mixtures of EOCs shed light on the contribution of each EOC against *S. aureus* and *P. aeruginosa*.

A relevant finding of the study was that carvacrol-loaded fibers were efficient against both bacteria, while fibers loaded with cinnamic acid solely were selective against the Gram-positive bacteria, which may be preferable when discriminating antimicrobial treatments are required. Fibers of carvacrol solely and its binary mixtures also showed suitable mechanical properties and antioxidant effects to perform as wound dressings. In fact, the human blood compatibility tests and the *in ovo* CAM assay highlighted the excellent biocompatibility of the developed fibers, which must be confirmed in vivo. A limitation of the study is related to the difficulty of mimicking in vitro the complex environment of an infected wound bed, and thus future studies should include testing carvacrol-loaded fibers in a biorelevant preclinical model.

Overall, the results obtained evidenced that by tuning the fibers composition it is possible to prepare environment-friendly, cost-effective, antibiotic-free antimicrobial wound dressings that might find an advantageous position in the arsenal against skin and soft tissue infections.

CRediT authorship contribution statement

Iago Gonzalez-Prada: Writing – review & editing, Writing – original draft, Software, Methodology, Investigation, Formal analysis, Data curation, Conceptualization. **Anabela Borges:** Writing – review & editing, Writing – original draft, Validation, Supervision, Software, Resources, Methodology, Formal analysis, Data curation. **Beatriz Santos-Torres:** Writing – review & editing, Methodology, Investigation, Formal analysis, Data curation. **Beatriz Magariños:** Writing – review & editing, Validation, Supervision, Resources, Funding acquisition, Formal analysis, Conceptualization. **Manuel Simões:** Writing – review & editing, Writing – original draft, Validation, Supervision, Resources, Funding acquisition, Formal analysis, Conceptualization. **Angel Concheiro:** Writing – review & editing, Writing – original draft, Visualization, Validation, Supervision, Software, Resources, Project administration, Methodology, Investigation, Funding acquisition, Formal analysis, Data curation, Conceptualization. **Carmen Alvarez-Lorenzo:** Writing – review & editing, Writing – original draft, Visualization, Validation, Supervision, Software, Resources, Project administration, Methodology, Investigation, Funding acquisition, Formal analysis, Data curation, Conceptualization.

Declaration of competing interest

The authors declare that they have no known competing financial interests or personal relationships that could have appeared to influence the work reported in this paper.

Data availability

Data will be made available on request.

Acknowledgements

I. Gonzalez-Prada acknowledges IACOBUS (Galicia-Northern Portugal European grouping program for territorial cooperation) fellowship for a three-months stay at the FEUP, University of Porto. A. Borges thanks the Portuguese Foundation for Science and Technology (FCT; Lisbon, Portugal) for the financial support of her work contract through the Scientific Employment Stimulus—Individual Call (CEECIND/00823/2021; DOI: 10.54499/2021.00823.CEECIND/CP1679/CT0014).

Funding

The work was supported by MCIN [PID 2020-113881RB-I00/AEI/10.13039/501100011033], Spain, FEDER and Xunta de Galicia [ED431C 2024/09]. The work was also partially granted by the Spanish Ministry of Science and Innovation with funds from the European Union NextGenerationEU, from the Recovery, Transformation and Resilience Plan (PRTR-C17.I1) and the Autonomous Community of Galicia within the framework of the Biotechnology Plan Applied to Health. This work was also partially supported by the European Commission (Horizon-Widera 2023-Access-02/Horizon-CSA) [InnovAntiBiofilm, ref. 101157363], and LEPABE, UIDB/00511/2020 [DOI: 10.54499/UIDB/00511/2020] and UIDP/00511/2020 [DOI: 10.54499/UIDP/00511/2020]; ALiCE, LA/P/0045/2020 [DOI: 10.54499/LA/P/0045/2020]; and the FCT/MCTES (PIDDAC; Lisbon, Portugal).

Appendix A. Supplementary data

Supplementary data to this article can be found online at https://doi.org/10.1016/j.ijbiomac.2024.134154.

References

[1] D. Nathwani, M. Dryden, J. Garau, Early clinical assessment of response to treatment of skin and soft-tissue infections: how can it help clinicians? Perspectives from Europe, Int. J. Antimicrob. Agents 48 (2016) 127–136, https://doi.org/10.1016/j.ijantimicag.2016.04.023.

[2] H.N. Leong, A. Kurup, M.Y. Tan, A.L.H. Kwa, K.H. Liau, M.H. Wilcox, Management of complicated skin and soft tissue infections with a special focus on the role of newer antibiotics, Infect. Drug Resist. 11 (2018) 1959–1974, https://doi.org/10.2147/IDR.S172366.

[3] B. Silverberg, A structured approach to skin and soft tissue infections (SSTIS) in an ambulatory setting, Clin. Pract. 11 (2021) 65–74, https://doi.org/10.3390/clinpract11010011.

[4] H.B. Fung, J.Y. Chang, S. Kuczynski, A practical guide to the treatment of complicated skin and soft tissue infections, Drugs 63 (2003) 1459–1480, https://doi.org/10.2165/00003495-200363140-00003.

[5] A.K. Tiwari, R. Lal, Study to evaluate the role of severity stratification of skin and soft tissue infections (SSTIs) in formulating treatment strategies and predicting poor prognostic factors, Int. J. Surg. 12 (2014) 125–133, https://doi.org/10.1016/j.ijsu.2013.11.014.

[6] M. Frieri, K. Kumar, A. Boutin, Antibiotic resistance, J. Infect. Public Health 10 (2017) 369–378, https://doi.org/10.1016/j.jiph.2016.08.007.

[7] Z. Yu, J. Tang, T. Khare, V. Kumar, The alarming antimicrobial resistance in ESKAPEE pathogens: can essential oils come to the rescue? Fitoterapia 140 (2020) 104433 https://doi.org/10.1016/j.fitote.2019.104433.

[8] U. Anand, N. Jacobo-Herrera, A. Altemimi, N. Lakhssassi, A comprehensive review on medicinal plants as antimicrobial therapeutics: potential avenues of biocompatible drug discovery, Metabolites 9 (2019) 1–13, https://doi.org/10.3390/metabo9110258.

[9] M. Raghavan, P.K. Linden, Newer treatment options for skin and soft tissue infections, Drugs 64 (2004) 1621–1642, https://doi.org/10.2165/00003495-200464150-00002.

[10] N.A. Turner, B.K. Sharma-Kuinkel, S.A. Maskarinec, E.M. Eichenberger, P.P. Shah, M. Carugati, T.L. Holland, V.G. Fowler Jr., Methicillin-resistant *Staphylococcus aureus*: an overview of basic and clinical research, Nat. Rev. Microbiol. 17 (2019) 203–218, https://doi.org/10.1038/s41579-018-0147-4.

[11] S. Santajit, N. Indrawattana, Mechanisms of antimicrobial resistance in ESKAPE pathogens, Biomed. Res. Int. 2016 (2016) 2475067, https://doi.org/10.1155/2016/2475067.
[12] S. Chouhan, K. Sharma, S. Guleria, Antimicrobial activity of some essential oils—present status and future perspectives, Medicines 4 (2017) 58, https://doi.org/10.3390/medicines4030058.
[13] M.K. Swamy, M.S. Akhtar, U.R. Sinniah, Antimicrobial properties of plant essential oils against human pathogens and their mode of action: an updated review, Evid. Based Complement. Alternat. Med. 2016 (2016) 3012462, https://doi.org/10.1155/2016/3012462.
[14] A. Bernardos, M. Bozik, S. Alvarez, M. Soskova, E. Perez-Esteve, P. Kloucek, M. Lhotka, A. Frankova, R. Martinez-Manez, The efficacy of essential oil components loaded into montmorillonite against *Aspergillus niger* and *Staphylococcus aureus*, flavour, Fragr. J. 34 (2019) 151–162, https://doi.org/10.1002/ffj.3488.
[15] P.L. Santos, J.P.S.C.F. Matos, L. Picot, J.R.G.S. Almeida, J.S.S. Quintans, L. J. Quintans-Júnior, Citronellol, a monoterpene alcohol with promising pharmacological activities - a systematic review, Food Chem. Toxicol. 123 (2019) 459–469, https://doi.org/10.1016/j.fct.2018.11.030.
[16] B. Melendez-Rodriguez, K.J. Figueroa-Lopez, A. Bernardos, R. Martínez-Máñez, L. Cabedo, S. Torres-Giner, J.M. Lagaron, Electrospun antimicrobial films of poly (3-hydroxybutyrate-co-3-hydroxyvalerate) containing eugenol essential oil encapsulated in mesoporous silica nanoparticles, Nanomaterials 9 (2019) 227, https://doi.org/10.3390/nano9020227.
[17] A. Radisavljevic, D.B. Stojanovic, S. Perisic, V. Djokic, V. Radojevic, M. Rajilic-Stojanovic, P.S. Uskokovic, Cefazolin-loaded polycaprolactone fibers produced via different electrospinning methods: characterization, drug release and antibacterial effect, Eur. J. Pharm. Sci. 124 (2018) 26–36, https://doi.org/10.1016/j.ejps.2018.08.023.
[18] X. Hu, S. Liu, G. Zhou, Y. Huang, Z. Xie, X. Jing, Electrospinning of polymeric nanofibers for drug delivery applications, J. Control. Release 185 (2014) 12–21, https://doi.org/10.1016/j.jconrel.2014.04.018.
[19] N. Bhardwaj, S.C. Kundu, Electrospinning: a fascinating fiber fabrication technique, Biotechnol. Adv. 28 (2010) 325–347, https://doi.org/10.1016/j.biotechadv.2010.01.004.
[20] F. Hemmati, A. Bahrami, A.F. Esfanjani, H. Hosseini, D.J. McClements, L. Williams, Electrospun antimicrobial materials: advanced packaging materials for food applications, Trends Food Sci. Technol. 111 (2021) 520–533, https://doi.org/10.1016/j.tifs.2021.03.014.
[21] Y. Li, Q. Meng, S. Chen, P. Ling, M.A. Kuss, B. Duan, S. Wu, Advances, challenges, and prospects for surgical suture materials, Acta Biomater. 168 (2023) 78–112, https://doi.org/10.1016/j.actbio.2023.07.041.
[22] F. Zhou, C. Cui, S. Sun, S. Wu, S. Chen, J. Ma, C.M. Li, Electrospun ZnO-loaded chitosan/PCL bilayer membranes with spatially designed structure for accelerated wound healing, Carbohydr. Polym. 282 (2022) 119131, https://doi.org/10.1016/j.carbpol.2022.119131.
[23] Z. Qu, Y. Wang, Y. Dong, X. Li, L. Hao, L. Sun, L. Zhou, R. Jiang, W. Liu, Intelligent electrospinning nanofibrous membranes for monitoring and promotion of the wound healing, Mater Today Bio. 26 (2024) 101093, https://doi.org/10.1016/j.mtbio.2024.101093.
[24] D. Mondal, M. Griffith, S.S. Venkatraman, Polycaprolactone-based biomaterials for tissue engineering and drug delivery: current scenario and challenges, Int. J. Polym. Mater. 65 (2016) 255–265, https://doi.org/10.1080/00914037.2015.1103241.
[25] G. Narayanan, R. Aguda, M. Hartman, C. Chung, R. Boy, B.S. Gupta, A.E. Tonelli, Fabrication and characterization of poly(ε-caprolactone)/α-cyclodextrin pseudorotaxane nanofibers, Biomacromolecules 17 (2016) 271–279, https://doi.org/10.1021/acs.biomac.5b01379.
[26] F. Topuz, T. Uyar, Electrospinning of cyclodextrin functional nanofibers for drug delivery applications, Pharmaceutics 11 (2019) 6, https://doi.org/10.3390/pharmaceutics11010006.
[27] F. Velázquez-Contreras, N. García-Caldera, J.D. Padilla de la Rosa, D. Martínez-Romero, E. Núñez-Delicado, J.A. Gabaldón, Effect of PLA active packaging containing monoterpene-cyclodextrin complexes on berries preservation, Polymers 13 (2021) 1399, https://doi.org/10.3390/polym13091399.
[28] G. Narayanan, B.S. Gupta, A.E. Tonelli, Enhanced mechanical properties of poly (ε-caprolactone) nanofibers produced by the addition of non-stoichiometric inclusion complexes of poly (ε-caprolactone) and α-cyclodextrin, Polymer 76 (2015) 321–330, https://doi.org/10.1016/j.polymer.2015.08.045.
[29] C. Alvarez-lorenzo, C.A. García-González, A. Concheiro, Cyclodextrins as versatile building blocks for regenerative medicine, J. Control. Release 268 (2017) 269–281, https://doi.org/10.1016/j.jconrel.2017.10.038.
[30] A. Costoya, A. Concheiro, C.A. Alvarez-Lorenzo, Electrospun fibers of cyclodextrins and poly(cyclodextrins), Molecules 22 (2017) 230, https://doi.org/10.3390/molecules22020230.
[31] M. Dias Antunes, G. da Silva Dannenberg, A.M. Fiorentini, V.Z. Pinto, L.T. Lim, E. da Rosa Zavareze, A.R.G. Dias, Antimicrobial electrospun ultrafine fibers from zein containing eucalyptus essential oil/cyclodextrin inclusion complex, Int. J. Biol. Macromol. 104 (2017) 874–882, https://doi.org/10.1016/j.ijbiomac.2017.06.095.
[32] Y. Liu, X. Liang, R. Zhang, W. Lan, W. Qin, Fabrication of electrospun polylactic acid/cinnamaldehyde/β-cyclodextrin fibers as an antimicrobial wound dressing, Polymers 9 (2017) 464, https://doi.org/10.3390/polym9100464.
[33] Z.I. Yildiz, A. Celebioglu, M.E. Kilic, E. Durgun, T. Uyar, Fast-dissolving carvacrol/cyclodextrin inclusion complex electrospun fibers with enhanced thermal stability, water solubility, and antioxidant activity, J. Mater. Sci. 53 (2018) 15837–15849, https://doi.org/10.1007/s10853-018-2750-1.
[34] Z.I. Yildiz, M.E. Kilic, E. Durgun, T. Uyar, Molecular encapsulation of cinnamaldehyde within cyclodextrin inclusion complex electrospun nanofibers: fast-dissolution, enhanced water solubility, high temperature stability, and antibacterial activity of cinnamaldehyde, J. Agric. Food Chem. 67 (2019) 11066–11076, https://doi.org/10.1021/acs.jafc.9b02789.
[35] L. Martins, C.E. dos Santos Cruxen, G. Pinheiro Bruni, A.M. Fiorentini, E. da Rosa Zavareze, L.T. Lim, A.R. Guerra Dias, Development of antimicrobial and antioxidant electrospun soluble potato starch nano fibers loaded with carvacrol, Int. J. Biol. Macromol. 139 (2019) 1182–1190, https://doi.org/10.1016/j.ijbiomac.2019.08.096.
[36] A. Nostro, A.R. Blanco, M.A. Cannatelli, V. Enea, G. Flamini, I. Morelli, A. S. Roccaro, V. Alonzo, Susceptibility of methicillin-resistant staphylococci to oregano essential oil, carvacrol and thymol, FEMS Microbiol. Lett. 230 (2004) 191–195, https://doi.org/10.1016/S0378-1097(03)00890-5.
[37] J.C. Lopez-Romero, H. González-Ríos, A. Borges, M. Simões, Antibacterial effects and mode of action of selected essential oils components against *Escherichia coli* and *Staphylococcus aureus*, Evid. Based Complement. Alternat. Med. 2015 (2015) 795435, https://doi.org/10.1155/2015/795435.
[38] N. Ruwizhi, B.A. Aderibigbe, Cinnamic acid derivatives and their biological efficacy, Int. J. Mol. Sci. 21 (2020) 5712, https://doi.org/10.3390/ijms21165712.
[39] J. Malheiro, I. Gomes, A. Borges, M.M.S.M. Bastos, J.Y. Maillard, F. Borges, M. Simões, Phytochemical profiling as a solution to palliate disinfectant limitations, Biofouling 32 (2016) 1007, https://doi.org/10.1080/08927014.2016.1220550.
[40] J.F. Malheiro, J.Y. Maillard, F. Borges, M. Simões, Evaluation of cinnamaldehyde and cinnamic acid derivatives in microbial growth control, Int. Biodeterior. Biodegrad. 141 (2019) 71–78, https://doi.org/10.1016/j.ibiod.2018.06.003.
[41] European Medicines Agency, Cyclodextrins used as excipients. https://www.ema.europa.eu/en/documents/scientific-guideline/questions-and-answers-cyclodextrins-used-excipients-medicinal-products-human-use_en.pdf, 2017.
[42] M. Ayaz, F. Ullah, A. Sadiq, F. Ullah, M. Ovais, J. Ahmed, H.P. Devkota, Synergistic interactions of phytochemicals with antimicrobial agents: potential strategy to counteract drug resistance, Chem. Biol. Interact. 308 (2019) 294–303, https://doi.org/10.1016/j.cbi.2019.05.050.
[43] I.M. Oliveira, A. Borges, F. Borges, M. Simões, Repurposing ibuprofen to control Staphylococcus aureus biofilms, Eur. J. Med. Chem. 166 (2019) 197–205, https://doi.org/10.1016/j.ejmech.2019.01.046.
[44] M.M. Leitão, T.F. Vieira, S.F. Sousa, F. Borges, M. Simões, A. Borges, Dual action of benzaldehydes: inhibiting quorum sensing and enhancing antibiotic efficacy for controlling *Pseudomonas aeruginosa* biofilms, Microb. Pathog. 191 (2024 Jun) 106663, https://doi.org/10.1016/j.micpath.2024.106663.
[45] C. Wiegand, T. Heinze, U.C. Hipler, Comparative in vitro study on cytotoxicity, antimicrobial activity, and binding capacity for pathophysiological factors in chronic wounds of alginate and silver-containing alginate, Wound Repair Regen. 17 (2009) 511–521, https://doi.org/10.1111/j.1524-475X.2009.00503.x.
[46] I.M. Oliveira, A. Borges, F. Borges, M. Simões, Repurposing ibuprofen to control *Staphylococcus aureus* biofilms, Eur. J. Med. Chem. 166 (2019) 197–205, https://doi.org/10.1016/j.ejmech.2019.01.046.
[47] A. Borges, C. Ferreira, M.J. Saavedra, M. Simões, Antibacterial activity and mode of action of ferulic and gallic acids against pathogenic bacteria, Microb. Drug Resist. 19 (2013) 256–265, https://doi.org/10.1089/mdr.2012.0244.
[48] C.J. van Oss, M.K. Chaudhury, R.J. Good, Monopolar surfaces, Adv. Colloid Interfac. 28 (1987) 35–64, https://doi.org/10.1016/0001-8686(87)80008-8.
[49] C.J. van Oss, R.J. Good, M.K. Chaudhury, Additive and nonadditive surface tension components and the interpretation of contact angles, Langmuir 4 (1988) 884–891, https://doi.org/10.1021/la00082a018.
[50] C.J. van Oss, L. Ju, M.K. Chaudhury, R.J. Good, Estimation of the polar parameters of the surface tension of liquids by contact angle measurements on gels, J. Colloid Interface Sci. 128 (1989) 313–319, https://doi.org/10.1016/0021-9797(89)90345-7.
[51] B. Janczuk, E. Chibowski, J.M. Bruque, M.L. Kerkeb, F.G. Caballero, On the consistency of surface free energy components as calculated from contact angles of different liquids: an application to the cholesterol surface, J. Colloid Interface Sci. 159 (1993) 421–428, https://doi.org/10.1006/jcis.1993.1342.
[52] A. Contreras-García, E. Bucio, A. Concheiro, C. Alvarez-Lorenzo, Polypropylene grafted with NIPAAm and APMA for creating hemocompatible surfaces that load/elute nalidixic acid, React. Funct. Polym. 70 (2010) 836–842, https://doi.org/10.1016/j.reactfunctpolym.2010.07.019.
[53] M.L. Ponce, H.K. Kleinmann, The chick chorioallantoic membrane as an in vivo angiogenesis model, Curr. Protoc. Cell Biol. 19 (2003) 1–6, https://doi.org/10.1002/0471143030.cb1905s1.
[54] B.R. Williamson, R. Krishnaswamy, A.E. Tonelli, Physical properties of poly (ε-caprolactone) coalesced from its α-cyclodextrin inclusion compound, Polymer 52 (2011) 4517–4527, https://doi.org/10.1016/j.polymer.2011.07.043.
[55] G. Narayanan, B.R. Ormond, B.S. Gupta, A.E. Tonelli, Efficient wound odor removal by β-cyclodextrin functionalized poly (ε-caprolactone) nanofibers, J. Appl. Polym. Sci. 132 (2015) 42782, https://doi.org/10.1002/app.42782.
[56] M. Gobin, R. Proust, S. Lack, L. Duciel, C. Des Courtils, E. Pauthe, A. Gand, D. Seyer, A combination of the natural molecules gallic acid and carvacrol eradicates *P. aeruginosa* and *S. aureus* mature biofilms, Int. J. Mol. Sci. 23 (2022) 7118, https://doi.org/10.3390/ijms23137118.
[57] K.S. Letsididi, Z. Lou, R. Letsididi, K. Mohammed, B.L. Maguy, Antimicrobial and antibiofilm effects of trans-cinnamic acid nanoemulsion and its potential

application on lettuce, LWT 94 (2018) 25–32, https://doi.org/10.1016/j.lwt.2018.04.018.
[58] C. Abril- Sánchez, A. Matencio, S. Navarro-Orcajada, F. García-Carmona, J. M. López-Nicolás, Evaluation of the properties of the essential oil citronellal nanoencapsulated by cyclodextrins, Chem. Phys. Lipids 219 (2019) 72–78, https://doi.org/10.1016/j.chemphyslip.2019.02.001.
[59] M.I. Rodríguez-López, M.T. Mercader-Ros, J.A. Pellicer, V.M. Gómez-López, D. Martínez-Romero, E. Núñez-Delicado, J.A. Gabaldón, Evaluation of monoterpene-cyclodextrin complexes as bacterial growth effective hurdles, Food Control 108 (2020) 106814, https://doi.org/10.1016/j.foodcont.2019.106814.
[60] K.J. Figueroa-Lopez, D. Enescu, S. Torres-Giner, L. Cabedo, M.A. Cerqueira, L. Pastrana, P. Fuciños, J.M. Lagaron, Development of electrospun active films of poly(3-hydroxybutyrate-co-3-hydroxyvalerate) by the incorporation of cyclodextrin inclusion complexes containing oregano essential oil, Food Hydrocoll. 108 (2020) 106013, https://doi.org/10.1016/j.foodhyd.2020.106013.
[61] M.H. Cavanagh, R.E. Burrell, P.L. Nadworny, Evaluating antimicrobial efficacy of new commercially available silver dressings, Int. Wound J. 7 (2010) 394–405, https://doi.org/10.1111/j.1742-481X.2010.00705.x.
[62] G. Mancuso, A. Midiri, E. Gerace, C. Biondo, Bacterial antibiotic resistance: the most critical pathogens, Pathogens 10 (2021) 1310, https://doi.org/10.3390/pathogens10101310.
[63] M.R. Tapia-Rodriguez, A. Hernandez-Mendoza, G.A. Gonzalez-Aguilar, M. A. Martinez-Tellez, C.M. Martins, J.F. Ayala-Zavala, Carvacrol as potential quorum sensing inhibitor of *Pseudomonas aeruginosa* and biofilm production on stainless steel surfaces, Food Control 75 (2017) 255–261, https://doi.org/10.1016/j.foodcont.2016.12.014.
[64] G. Brackman, M.J. Garcia-Fernandez, J. Lenoir, L. De Meyer, J.P. Remon, T. De Beer, A. Concheiro, C. Alvarez-Lorenzo, T. Coenye, Dressings loaded with cyclodextrin-hamamelitannin complexes increase *Staphylococcus aureus* susceptibility toward antibiotics both in single as well as in mixed biofilm communities, Macromol. Biosci. 16 (2016) 859–869, https://doi.org/10.1002/mabi.201500437.
[65] M. Duplantier, E. Lohou, P. Sonnet, Quorum sensing inhibitors to quench *P. aeruginosa* pathogenicity, Pharmaceuticals 14 (2021) 1262, https://doi.org/10.3390/ph14121262.
[66] Z. Berkl, I. Fekete-Kertész, K. Buda, E. Vaszita, E. Fenyvesi, L. Szente, M. Molnár, Effect of cyclodextrins on the biofilm formation capacity of *Pseudomonas aeruginosa* PAO1, Molecules 27 (2022) 3603, https://doi.org/10.3390/molecules27113603.
[67] T.K. Dash, V.B. Konkimalla, Poly-ϵ-caprolactone based formulations for drug delivery and tissue engineering: a review, J. Control. Release 158 (2012) 15–33, https://doi.org/10.1016/j.jconrel.2011.09.064.
[68] M.W. Tackenberg, C. Geisthövel, A. Marmann, H.P. Schuchmann, P. Kleinebudde, M. Thommes, Mechanistic study of carvacrol processing and stabilization as glassy solid solution and microcapsule, Int. J. Pharm. 478 (2015) 597–605, https://doi.org/10.1016/j.ijpharm.2014.12.012.
[69] F. Menicucci, E. Palagano, M. Michelozzi, G. Cencetti, A. Raio, A. Bacchi, P. P. Mazzeo, O.A. Cuzman, A. Sidoti, S. Guarino, S. Basile, O. Riccobono, E. Peri, F. Vizza, A. Ienco, Effects of trapped-into-solids volatile organic compounds on paper biodeteriogens, Int. Biodeter. Biodegr. 174 (2022) 105469, https://doi.org/10.1016/j.ibiod.2022.105469.
[70] A.R. Albunia, P. Rizzo, G. Ianniello, C. Rufolo, G. Guerra, Syndiotactic polystyrene films with a cocrystalline phase including carvacrol guest molecules, J Polym Sci B 52 (2014) 657–665, https://doi.org/10.1002/polb.23464.
[71] G. Narayanan, B.S. Gupta, A. Tonelli, Poly(ε-caprolactone) nanowebs functionalized with α- and γ-cyclodextrins, Biomacromolecules 15 (2014) 4122–4133, https://doi.org/10.1021/bm501158w.
[72] M. Lemos, A. Borges, J. Teodósio, P. Araújo, F. Mergulhão, L. Melo, M. Simões, The effects of ferulic and salicylic acids on *Bacillus cereus* and *Pseudomonas fluorescens* single- and dual-species biofilms, Int. Biodeter. Biodegr. 86 (2014) 42–51, https://doi.org/10.1016/j.ibiod.2013.06.011.
[73] S. López-Miranda, D. Berdejo, E. Pagán, D. García-Gonzalo, R. Pagán, Modified cyclodextrin type and dehydration methods exert a significant effect on the antimicrobial activity of encapsulated carvacrol and thymol, J. Sci. Food Agric. 101 (2021) 3827–3835, https://doi.org/10.1002/jsfa.11017.
[74] D. Ribatti, The chick embryo chorioallantoic membrane (CAM). A multifaceted experimental model, Mech. Dev. 141 (2016) 70–77, https://doi.org/10.1016/j.mod.2016.05.003.
[75] X. Farto-Vaamonde, L. Diaz-Gomez, A. Parga, A. Otero, A. Concheiro, C. Alvarez-Lorenzo, Perimeter and carvacrol-loading regulate angiogenesis and biofilm growth in 3D printed PLA scaffolds, J. Control. Release 352 (2022) 776–792, https://doi.org/10.1016/j.jconrel.2022.10.060.
[76] D.Y. Choi, Y.H. Baek, J.E. Huh, J.M. Ko, H.S. Woo, J.D. Lee, D.S. Park, Stimulatory effect of *Cinnamomum cassia* and cinnamic acid on angiogenesis through up-regulation of VEGF and Flk-1/KDR expression, Int. Immunopharmacol. 9 (2009) 959–967.
[77] D. Matluobi, A. Araghi, B.F.A. Maragheh, A. Rezabakhsh, S. Soltani, M. Khaksar, V. Siavashi, A. Feyzi, H.S. Bagheri, R. Rahbarghazi, S. Montazersaheb, Carvacrol promotes angiogenic paracrine potential and endothelial differentiation of human mesenchymal stem cells at low concentrations, Microvasc. Res. 115 (2018) 20–27, https://doi.org/10.1016/j.mvr.2017.08.003.